202000-11-T

Technical Report—Study Service Contract

TASK 1: AUTOMATED GADS FEASIBILITY

Environmental Research Institute of Michigan
Image Processing Systems Division
P.O. Box 8618
Ann Arbor, MI 48107-8618

APRIL 1988

(Period September 1987—March 1988)

Department of the Air Force
Armament Division
Eglin AFB, FL 32542-5320
F08635-87-C-0074

ERIM P.O. Box 8618 Ann Arbor, MI 48107-8618

REPORT DOCUMENTATION PAGE

Form Approved
OMB No. 0704-0188

1a REPORT SECURITY CLASSIFICATION Unclassified	1b RESTRICTIVE MARKINGS
2a SECURITY CLASSIFICATION AUTHORITY	3 DISTRIBUTION/AVAILABILITY OF REPORT [redacted]
2b DECLASSIFICATION/DOWNGRADING SCHEDULE	
4 PERFORMING ORGANIZATION REPORT NUMBERS(S)	5 MONITORING ORGANIZATION REPORT NUMBER(S)
6a NAME OF PERFORMING ORGANIZATION Environmental Research Institute of Michigan 6b OFFICE SYMBOL (if applicable)	7a NAME OF MONITORING ORGANIZATION Department of the Air Force Armament Division
6c ADDRESS (City, State, and ZIP Code) P.O. Box 8618 Ann Arbor, MI 48107-8618	7b ADDRESS (City, State, and ZIP Code) AD/KRT Eglin AFB, FL 32542-5320
8a NAME OF FUNDING /SPONSORING ORGANIZATION Department of the Air Force Armament Division 8b OFFICE SYMBOL (if applicable)	9 PROCUREMENT INSTRUMENT IDENTIFICATION NUMBER F08635-87-C-0074
8c ADDRESS (City, State, and ZIP Code) AD/KRT Eglin AFB, FL 32542-5320	10 SOURCE OF FUNDING NUMBERS PROGRAM ELEMENT NO / PROJECT NO / TASK NO / WORK UNIT ACCESSION NO
11 TITLE (Include Security Classification) Automated GADS Feasibility	
12 PERSONAL AUTHOR(S) Charles D. Lake, Dr. James W. Sherman	
13a TYPE OF REPORT Technical	13b TIME COVERED FROM 9/1/87 TO 3/31/88
14 DATE OF REPORT (Year, Month, Day) 4/11/88	15 PAGE COUNT 48
16 SUPPLEMENTARY NOTATION	

17 COSATI CODES			18 SUBJECT TERMS (Continue on reverse if necessary and identify by block number)
FIELD	GROUP	SUB-GROUP	

19 ABSTRACT (Continue on reverse if necessary and identify by block number)

The following technical report gives the results of a feasibility study for automatic Graphic Attitude Determination System (GADS) processing.

A prototype algorithm utilizing distance potential fields was developed for matching wireframe model data to single frames of short focal length imagery.

Encouraging results were obtained for estimating the six degrees of freedom for target position and attitude.

20 DISTRIBUTION/AVAILABILITY OF ABSTRACT X UNCLASSIFIED/UNLIMITED ☐ SAME AS RPT ☐ DTIC USERS	21 ABSTRACT SECURITY CLASSIFICATION Unclassified
22a NAME OF RESPONSIBLE INDIVIDUAL James W. Sherman	22b TELEPHONE (Include Area Code) (313) 994-1200 x2829 22c OFFICE SYMBOL

TABLE OF CONTENTS

LIST OF FIGURES

1.0 INTRODUCTION

GADS is the Graphic Attitude Determination System currently in use at Eglin Air Force Base for manually "reducing stores separation data from 16mm film." This process involves the manual matching of a wireframe model to the projected image of the weapon for each frame of the film. Using the information from the matched wireframe model, the camera location and optical characteristics, it is possible to determine the position of the store as a function of time. While the technique has been very successful, it is labor intensive and a fatiguing process for the operator. Manual operation also raises the challenge of consistent matching within a film sequence and between operators. Finally, a quantitative criteria for determining model position cannot be assessed with the present manual system. As such, assistance for the operator in the form of additional information, options on how information is presented, and ideally an automatic matching capability is highly desirable. This paper outlines upgrades to the manual operation at the algorithmic level, focussing on the feasibility of automatically matching model data to images from film.

2.0 LITERATURE REVIEW

An extensive literature search was undertaken at the beginning of this project to assess the applicability of recent research to the problems posed by automated GADS. The details of this survey are included in Appendix A. From the several hundred titles of potential relevance, over 20 articles were requested and reviewed. While some of the techniques discussed could be beneficial in portions of a final automated algorithm, most were extremely specific and restrictive in the problem addressed and the solution tendered.

In the GADS environment, model matching occurs on noisy images with obscured moving targets taken from a nonstationary camera under highly variable lighting conditions and target backgrounds. This scenario provides a rich source of topics, but few of the papers examined dealt with more than one or two of the simultaneous concert of conditions in GADS. The previous research of greatest benefit was discovered at the IEEE Sixteenth Workshop on Applied Imagery Pattern Recognition held October 28-30, 1987, in Washington, D.C., attended by ERIM representatives including this project's program manager, Dr. James Sherman. A. S. Politopoulos presented a paper on ATR recognition with a technique for correlation of 2 line models using a minimum distance metric. From this kernel idea, the use of "potential fields" was developed and incorporated in the design of an automatic algorithm.

3.0 ALGORITHM OVERVIEW

ERIM advocates an evolutionary, incremental approach to developing an automated GADS capability, building on the experience gained from manual operations and utilizing existing hardware and techniques *as appropriate*. From an operator's viewpoint, an automated

GADS system would be the same as the manual GADS system with the addition of some menu options to provide automatic matching of the wireframe model to the image data. In this approach, the operator has the capability of switching between automatic and manual matching at any time. Information similar to that utilized for automatic model placement would also be optionally available to aid the operator in manual mode and in quantitatively assessing the model fit to the image. The basic sequence for automatic mode is as follows:

(1) An operator initializes the system by selecting the first frame, appropriate model, and positioning the model "close enough" to the target before selecting automatic processing.

(2) The algorithm extracts features from the image with correspondence to features in target model, e.g., for wireframe models, edges would be extracted from the image.

(3) A "potential field" is generated around the target model.
Note that the location would be the operator positioned model for initialization, the previous frame's final model position for the start of the next frame, (optionally modified by autoprediction), or a candidate model position when iterating for a best fit.

(4) The extracted image features are placed in the model's "potential field" and the "gravitational forces" acting on the features are calculated. Topographically, the model forms a valley with mountains of constant slope on all sides. When the image features are placed in this terrain, they will slide down towards the valley until the lowest possible position is reached.

(5) The information obtained from step 4 is used to shift the target model so as to minimize the "forces" acting on the image features from the model "potential field." Because this is an approximate positioning, the algorithm loops back to step 3 and iterates until an overall minimum is achieved.

(6) The algorithm outputs the results of the model fit, including a confidence measure for each of the 6 degrees of freedom reported.

(7) Finally, the algorithm determines the next frame in the sequence (if any), digitizes the image, and repeats the matching process starting at step 2. Note that the next frame may be forward or backward in time, may be more than one frame distant, or may be selected by the operator.

Throughout this sequence, the operator retains the option of extensive review and veto powers over the model placement. It will be possible to interrupt automatic model positioning, reposition the model manually, and restart automatic mode from the manual placement. The initial model position being "close enough" refers to placement that leads to closure on the best fit. Currently, it's unlikely the algorithm will close to the proper model fit given an initial rotation of 45° or more from truth for yaw and pitch and 22° for roll. While it's anticipated that this restriction will be minor, "close enough" is a function of the model, its orientation, and the imagery being processed. As such, *no single number* bounding "close enough" is possible without restricting other system parameters. Consider the extreme case

of a bomb largely obscured by the aircraft with the exposed portion completely obscured (for a single frame) by vapor. In this instance "close enough" doesn't exist, and the algorithm would firmly request the operator to select a different frame for initialization.

4.0 CRITICAL ALGORITHM COMPONENTS

In the development of a new algorithm, a scale of feasibility risk will evolve for various portions of the approach. To assure the overall validity of an approach, the highest risk sections of an algorithm must be selected and developed. In this instance, the precise matching of image features to model data was of greatest concern to ERIM staff. Accordingly, steps 3-5 were identified as those of a critical nature and were developed and demonstrated to Eglin personnel. Of central importance to the matching technique was the development of an appropriate field of values around the model data. The fields used are fully discussed in the Model Field Potential section. Technical details on how matching is accomplished are given in the Algorithm Calculation section. ERIM's focus on feature matching to model data should not be construed as trivializing the other steps in the algorithm. In particular, extraction of features from the image, step 2, represents a significant challenge. From the results of these efforts, ERIM is confident of the overall feasibility of an automated GADS system.

5.0 MODEL POTENTIAL FIELD

In the automated GADS environment, exact correspondence between model pixels and image pixels is unknown, and initial model placement in the image data is only approximate. The feature data extracted from the image can be expected to contain noise, and not to contain features in desired locations due to a variety of factors including obscuration and lighting variations. As such, a correlation technique which is relatively insensitive to these factors needed to be developed. Drawing upon the analogy of gravitational or electromagnetic fields, ERIM developed a potential field which gives the distance to the nearest pixel on the model. That is, the field answers the question of how many lines and columns away is a model pixel as a function of location in the image.

The pixel neighborhood operations used to generate the fields are shown in Figure 1. The distance field consisting of both horizontal (dx) and vertical (dy) components gives the *total* number of x and y shifts to the closest model pixel. This scalar field, or composite potential field, is shown in the perspective plot of Figure 2, where the "model" source is simply two intersecting line segments. The dx field calculation shown in Figure 1 gives the magnitude of the horizontal component of the potential field. Similarly, the vertical field calculations are given with the dy kernal of Figure 1. These component fields are used in the feasibility algorithm to independently determine the line and column shift. In other words, the horizontal field gives the distance to the nearest model pixel in x. Concomitantly,

the vertical field gives the line distance for the minimum shift to a model pixel. Use of component fields helped simplify the algorithm calculations, but required more effort to develop an intuition concerning their correctness than the familiar topology of a potential field. For example, is the vertical band of zeroes in the dx field of Figure 1 correct? It would appear all the dx field values originate solely from the endpoints of the model. In this instance, the band of zeroes indicate that *no shift in x* is required to reach the nearest model pixel, i.e., the nearest model pixel can be reached with only vertical shifts. The horizontal and vertical components of the potential field in Figure 2 are shown in Figures 3 and 4. Again, these component fields do not correspond to intuition given the topology of the potential field in Figure 2.

When working with these prototype fields, an interesting situation arises. What happens when the *total shift*, as given by the potential field, gives more than one path to a model pixel? Consider a 45° line and a field pixel diagonally adjacent to this line. In such a case, the total number of shifts needed to reach the source line is two. Unfortunately, any one of three shift combinations give a path to the line: 2 shifts in y, 1 shift in y plus 1 in x, or 2 shifts in x. The prototype fields attempt to address this situation by giving the unambiguous portion of the shift. This results in pixels being moved to locations where they are equally unresistant to shifts in either direction. Our presumption is that pixels with unambiguous paths would provide the final push to align model and feature data. Anyone with an analytic mind should now be smiling at the thought of pathologic cases. Careful examination of the component fields in Figures 3 and 4 compared with the potential field of Figure 2 will reveal such a pathologic case. Notice the area inside the model lines has no horizontal or vertical field component. This arises from the fact that any pixel inside that region can reach a model pixel by more than one equidistant combination of shifts. While these prototype fields were sufficient for assessing feasibility, it's apparent that further work will be needed to satisfy the performance requirements in an automated GADS environment.

6.0 EXAMPLE SEQUENCE

Figures 5 through 17 provide a pictorial example for most of the steps in the algorithm overview. Figure 5 simply provides an example frame from a filmed drop as might be selected by an operator during initialization. Note that this image was not acquired by the equipment used in manual GADS. Images from manual GADS will provide improved quality. Step 2 in the algorithm is dramatized in Figures 6 through 8, in which features are extracted and refined. The "idealized feature extraction" in Figure 8 used model generated data. Use of model generated data for feature matching enabled ERIM staff to focus on the correlation problem and provided an unequivocal criteria for best fit, i.e., the two models should ultimately match *perfectly*.

Figure 9 gives a hypothetical start condition, which is a"close enough" placement of the model (shown in green) relative to the image features (shown in red). This example uses four of six degrees of freedom where the start position reflects a displacement in x, y, z, and

pitch. The out-of-plane angles, in this case yaw and roll, were not disturbed nor were they permitted to change in the iterations. Figures 10 and 11 show the horizontal and vertical components of the potential field corresponding to step 3 in the algorithm overview. The use of color in the fields is simply for visual aid in determining distance. Small distances are colored red, furthest are colored violet, and the isobar bands of blue are given every 10 pixels.

Algorithm step 4 is shown in Figures 12 and 13 where the image features are placed in the model's potential field and analyzed. For the horizontal field, 171 pixels require an addition to their column location, i.e., a shift right, while 227 pixels are voting for a left shift and 332 have a zero distance shift. Close examination of Figure 13 shows 20 pixels voting to shift *down*, while another 31 extend beyond the field. Both of these conditions represent violations of "close enough" model placement for the current algorithm. Counting the blue isobar lines reveals that the 20 green feature pixels in Figure 13 are greater than 127 pixels distant from the model. Since shifts are stored as signed 8-bit quantities, this results in the 20 pixels changing sign and voting for a large shift in the wrong direction. In this instance, the cumulative voting of the image feature pixels was still able to provide a stable response.

The results of the first iteration are shown in Figure 14 and correspond to step 5 in the algorithm overview. The model is shifted using a least squares calculation from the image feature data placed in the potential field. Considering the correct correlation is unknown, model placement is only approximate and the process must be repeated.

Figures 15 through 17 give the results for the 20^{th} iteration. Figure 17 contains the history of model placement in each iteration and reveals how rapidly the model closes upon image features. Finally, Figures 18 through 21 give a graphical analysis of model placement relative to feature location.

7.0 ALGORITHM INPUTS

An automated GADS capability will require several inputs, the majority of which are identical to those of manual GADS. The main inputs of interest for both systems are listed below:

- Target model data
- Digitized imagery
- Operator requests

Automated GADS will input model data by calling the program for generating wireframe models in the manual GADS operation. Utilization of existing software and techniques has an obvious cost benefit, assuming the following conditions are met:

- An interface between the model generated data and an automated GADS system can be accomplished with minimal effort. ERIM fully expects this to be the case.

- The wireframe data correlates with edges in the digitized imagery at a level sufficient to meet accuracy requirements.

Modifications to implement hidden line removal will be required given that this data is obscured in the real images (e.g., there are no edges for fins on the far side of the missile). While early studies support optimism for correlation of edges to the wireframe model, improved contrast and accuracy may be required. Utilization of imagery obtained through color filters matched to the film response will be explored as appropriate to assess the impact on system accuracy.

Digitized imagery from the manual GADS system will be processed for automated operations. While this is an obvious input, it is mentioned here to emphasize the need for a *standard* set of images by which the automated processing will be evaluated. It is recommended that personnel at Eglin select a representative set of filmed drops to provide a basis for evaluation of the algorithm results. The set of *digital* images needs to span the range of imaging conditions over which the algorithm performance will be evaluated.

Operator interactions are of two forms: those inputs requested by the automated GADS system, and requests initiated by the operator. The minimum algorithm inputs anticipated are selection of the first image frame, the target model, and initial placement of the model within the first frame. This operation is envisioned as identical to manual GADS operations with the additional option of shifting into automatic when the model is sufficiently close to the target. Given a "close enough" placement of the model, the automatic mode would perform the closing match to the target. After initialization, the operator always has the option of switching between manual and automatic model placement at any time and on any frame. When in automatic mode, the operator may optionally approve or reject the final model placement before the location results are logged.

8.0 ALGORITHM OUTPUTS

In the upgraded GADS system, the outputs will be identical whether from automatic or manual placement of the model. In particular, the following outputs are anticipated:

- Model location in x,y,z,yaw,pitch,roll
- Covariance matrix from error analysis (optional)
- Display of the image and model placement (optional in automatic mode)
- Various alphanumeric information to a terminal (same display for manual or automatic)

The model location values are those currently in use by manual GADS. The covariance matrix would reflect the coupling of errors between the various degrees of freedom and could be used in a Kalman filtering process. Calculation of this matrix will also reflect the strength of image features (edges) and their correlation with the model data. Finally, the last two

outputs mentioned emphasize the close relationship between manual and automatic modes. As previously mentioned, automatic mode is simply an option the operator invokes (or cancels) when running the GADS program. Notice that this upgrade optionally provides the operator numerical feedback on the manual placement of the model before location values are logged. Given that this approach is essentially an extension of the current manual operations, this effort has been locally referred to as the Enhanced Graphics Attitude Determination System or, alternatively, the Graphics Attitude Determination System Utilizing Knowledge Enhancement Services.

9.0 ALGORITHM CALCULATIONS

From the distance field generated for the model, we know the amount to shift in lines and columns to align a given feature image pixel with the nearest model pixel. These shifts are a function of pixel location and can be represented as a transformation between the coordinates of the feature image and the model image. Using a homogeneous coordinate system to facilitate matrix representation of translation and perspective, the transformation was represented as follows:

$$\begin{bmatrix} wu \\ wv \\ w \end{bmatrix} = \begin{bmatrix} \alpha & 0 & 0 \\ 0 & \alpha & 0 \\ p_1 & p_2 & 1 \end{bmatrix} \cdot \begin{bmatrix} c_\psi & -s_\psi & t_x \\ s_\psi & c_\psi & t_y \\ 0 & 0 & 1 \end{bmatrix} \cdot \begin{bmatrix} x \\ y \\ 1 \end{bmatrix} = \begin{bmatrix} \alpha c_\psi & -\alpha s_\psi & \alpha t_x \\ \alpha s_\psi & \alpha c_\psi & \alpha t_y \\ P_1 & P_2 & 1^* \end{bmatrix} \cdot \begin{bmatrix} x \\ y \\ 1 \end{bmatrix}$$

$$\begin{aligned} wu &= x\alpha c_\psi - y\alpha s_\psi + \alpha t_x \\ wv &= x\alpha s_\psi - y\alpha c_\psi + \alpha t_y \\ w &= xP_1 + yP_2 + 1^* \end{aligned} \quad \Longrightarrow \quad \begin{bmatrix} u \\ v \end{bmatrix} = \begin{bmatrix} 1 & 0 & x & -y & -xu & -yu \\ 0 & 1 & y & x & -xv & -yv \end{bmatrix} \cdot \begin{bmatrix} \alpha t_x \\ \alpha t_y \\ \alpha c_\psi \\ \alpha s_\psi \\ P_1 \\ P_2 \end{bmatrix}$$

$$\begin{aligned} p_1 &= \frac{-\alpha}{d}(s_\kappa s_\gamma) & P_1 &= \frac{\alpha}{d}[s_\psi(c_\kappa s_\gamma) - c_\psi(s_\kappa s_\gamma)] \\ p_2 &= \frac{\alpha}{d}(c_\kappa s_\gamma) & P_2 &= \frac{\alpha}{d}[s_\psi(s_\kappa s_\gamma) + c_\psi(c_\kappa s_\gamma)] \\ 1^* &= 1 + (t_y p_2 - t_x p_1) & \text{Note: } \lim_{t_x, t_y \to 0} 1^* &= \lim_{\gamma \to 0} 1^* = 1 \end{aligned}$$

The equations for determining the final coefficients use the value 1 in place of 1^*, i.e., we assume either translation is small, perspective change is small, or that: $t_y p_2 \approx t_x p_1$

Symbol definitions for this set of equations are as follows:

u Transformed (new) image column location

v	Transformed (new) image line location
w	Scale of homogeneous solution, result vector is divided by w to get u, v.
x	Original column position in the image
y	Original line location in the image
t_x	Number of columns (pixels) to translate
t_y	Number of rows (lines) to translate
α	Change in scale, i.e., Z_{new}/Z_{old}
ψ	The angle of *in the plane* image rotation, *counterclockwise from x*
γ	The angle of *out of plane* image rotation
κ	The in plane angle to the out of plane rotational axis, *counterclockwise from u*
c_ψ, s_ψ	Respectively, the cosine and sine of ψ
d	The distance from the focal plane to the image plane *in units of pixels*
p_1, p_2	Initial perspective terms
P_1, P_2	Final tranform perspective terms

The coefficients of the transformation are obtained from a weighted least squares solution to the large set of simultaneous equations for the pixel-to-pixel correspondences. The weighting allows the strength of the feature and other image properties to influence the solution. With this approach, we are solving for the translation of image features to the wireframe model. In the application, this transformation must be inverted to provide for the manipulation of the wireframe model.

We solved for object points to model points, but we need the model to object transformation

$$\overbrace{\begin{bmatrix} wu \\ wv \\ w \end{bmatrix} = \begin{bmatrix} \alpha c_\psi & -\alpha s_\psi & \alpha t_x \\ \alpha s_\psi & \alpha c_\psi & \alpha t_y \\ P_1 & P_2 & 1 \end{bmatrix} \cdot \begin{bmatrix} x \\ y \\ 1 \end{bmatrix}}^{} \longrightarrow \overbrace{\begin{bmatrix} w'x \\ w'y \\ w' \end{bmatrix} = \begin{bmatrix} \alpha' c_{\psi'} & -\alpha' s_{\psi'} & \alpha' t'_x \\ \alpha' s_{\psi'} & \alpha' c_{\psi'} & \alpha' t'_y \\ P'_1 & P'_2 & 1 \end{bmatrix} \cdot \begin{bmatrix} u \\ v \\ 1 \end{bmatrix}}$$

Let

$$\begin{bmatrix} \overbrace{w\begin{bmatrix} u \\ v \end{bmatrix}}^{\vec{m}} \\ w \end{bmatrix} = \begin{bmatrix} \overbrace{\begin{bmatrix} \alpha c_\psi & -\alpha s_\psi \\ \alpha s_\psi & \alpha c_\psi \end{bmatrix}}^{A} & \overbrace{\begin{bmatrix} \alpha t_x \\ \alpha t_y \end{bmatrix}}^{T} \\ \underbrace{\begin{bmatrix} P_1 & P_2 \end{bmatrix}}_{P} & 1 \end{bmatrix} \cdot \begin{bmatrix} \overbrace{\begin{bmatrix} x \\ y \end{bmatrix}}^{\vec{o}} \\ 1 \end{bmatrix}$$

then

$$\begin{bmatrix} w\vec{m} \\ w \end{bmatrix} = \begin{bmatrix} A & T \\ P & 1 \end{bmatrix} \cdot \begin{bmatrix} \vec{o} \\ 1 \end{bmatrix}$$

and similarly $$\begin{bmatrix} w'\vec{o} \\ w' \end{bmatrix} = \begin{bmatrix} A' & T' \\ P' & 1 \end{bmatrix} \cdot \begin{bmatrix} \vec{m} \\ 1 \end{bmatrix}$$

$$\left.\begin{aligned} w'\vec{o} &= A'\vec{m} + T' \\ w' &= 1 + P'\vec{m} \end{aligned}\right\} \longrightarrow \quad \vec{o} = \frac{A'\vec{m} + T'}{1 + P'\vec{m}} = \frac{A'\left(\frac{A\vec{o}+T}{1+P\vec{o}}\right) + T'}{1 + P'\left(\frac{A\vec{o}+T}{1+P\vec{o}}\right)} = \frac{A'(A\vec{o}+T) + T'(1+P\vec{o})}{1 + P\vec{o} + P'(A\vec{o}+T)}$$

Gathering terms yields $$\vec{o} = \frac{(A'A + T'P)\vec{o} + \overbrace{(A'T + T')}^{\text{Set to 0}}}{\underbrace{(P + P'A)}_{\text{Set to 0}}\vec{o} + (1 + P'T)} \quad \Rightarrow \quad \overbrace{\left(\frac{A'A + T'P}{1 + P'T}\right)}^{\text{Set to I}}\vec{o}$$

Solving $$A'T + T' = 0 \rightarrow T' = -A'T \qquad P + P'A = 0 \rightarrow P' = -PA^{-1}$$

From $$\frac{A'A + T'P}{1 + P'T}\vec{o} = I\vec{o}$$

$$A'A + T'P = I(1 + P'T)$$

Substitution gives $$A'A + (-A'T)P = I(1 + (-PA^{-1})T)$$

Postmultiply by A^{-1} $$A' - A'TPA^{-1} = A^{-1}(1 - PA^{-1}T)$$

$$A'(I - TPA^{-1}) = A^{-1}(1 - PA^{-1}T)$$

$$A' = A^{-1}(I - TPA^{-1})^{-1}(1 - PA^{-1}T)$$

For small translations or small *changes* in perspective, we can assume

$$A' \approx A^{-1} = \begin{bmatrix} \frac{c_\psi}{\alpha} & \frac{s_\psi}{\alpha} \\ \frac{-s_\psi}{\alpha} & \frac{c_\psi}{\alpha} \end{bmatrix} = \frac{1}{\alpha}\begin{bmatrix} c_\psi & s_\psi \\ -s_\psi & c_\psi \end{bmatrix}$$

Using this approximation, we can solve for P' and T'.

$$T' = -A'T = \frac{-1}{\alpha}\begin{bmatrix} c_\psi & s_\psi \\ -s_\psi & c_\psi \end{bmatrix}\begin{bmatrix} \alpha t_x \\ \alpha t_y \end{bmatrix} = \begin{bmatrix} -c_\psi t_x - s_\psi t_y \\ s_\psi t_x - c_\psi t_y \end{bmatrix}$$

$$P' = -PA^{-1} = \frac{-1}{\alpha}\begin{bmatrix} \mathrm{P}_1 & \mathrm{P}_2 \end{bmatrix}\begin{bmatrix} c_\psi & s_\psi \\ -s_\psi & c_\psi \end{bmatrix} = \frac{-1}{\alpha}\begin{bmatrix} (\mathrm{P}_1 c_\psi - \mathrm{P}_2 s_\psi) & (\mathrm{P}_1 s_\psi + \mathrm{P}_2 c_\psi) \end{bmatrix}$$

Solving for the individual terms in P'

$$\begin{aligned} P'_{11} &= \frac{-1}{\alpha}(\mathrm{P}_1 c_\psi - \mathrm{P}_2 s_\psi) \\ &= \frac{-1}{\alpha}\left(\frac{\alpha c_\psi}{\mathrm{d}}(s_\psi(c_\kappa s_\gamma) - c_\psi(s_\kappa s_\gamma)) - \frac{\alpha s_\psi}{\mathrm{d}}(c_\psi(c_\kappa s_\gamma) + s_\psi(s_\kappa s_\gamma))\right) \\ &= \frac{-1}{\mathrm{d}}\left(c_\psi s_\psi(c_\kappa s_\gamma) - c_\psi^2(s_\kappa s_\gamma) - s_\psi c_\psi(c_\kappa s_\gamma) - s_\psi^2(s_\kappa s_\gamma)\right) \\ &= \frac{s_\kappa s_\gamma}{\mathrm{d}} \end{aligned}$$

Similarly

$$
\begin{aligned}
P'_{12} &= \frac{-1}{\alpha}(\mathrm{P}_1 s_\psi + \mathrm{P}_2 c_\psi) \\
&= \frac{-1}{\alpha}\left(\frac{\alpha s_\psi}{\mathrm{d}}\left(s_\psi(c_\kappa s_\gamma) - c_\psi(s_\kappa s_\gamma)\right) + \frac{\alpha c_\psi}{\mathrm{d}}\left(c_\psi(c_\kappa s_\gamma) + s_\psi(s_\kappa s_\gamma)\right)\right) \\
&= \frac{-1}{\mathrm{d}}\left(s_\psi^2(c_\kappa s_\gamma) - s_\psi c_\psi(s_\kappa s_\gamma) + c_\psi^2(c_\kappa s_\gamma) + c_\psi s_\psi(s_\kappa s_\gamma)\right) \\
&= \frac{-c_\kappa s_\gamma}{\mathrm{d}}
\end{aligned}
$$

Thus,

$$
P' = \left[\begin{array}{cc} \frac{s_\kappa s_\gamma}{\mathrm{d}} & \frac{-c_\kappa s_\gamma}{\mathrm{d}} \end{array}\right] = \frac{s_\gamma}{\mathrm{d}}\left[\begin{array}{cc} s_\kappa & -c_\kappa \end{array}\right]
$$

The transformations utilized by the model generation program must be compensated for when calculating input to the wireframe model. In addition, the model parameter inputs must be the total or cumulative position rather than incremental changes obtained from the above calculations. The transformations used in model generation are as follows:

$\mathrm{Q_{mat}} = \text{translate} \cdot (\,(\text{roll} \cdot \text{pitch}) \cdot \text{yaw}\,)$ **Note: Multiplication is associative**

$$
\overbrace{\begin{bmatrix} 1 & 0 & 0 & t_x \\ 0 & 1 & 0 & t_y \\ 0 & 0 & 1 & t_z \\ 0 & 0 & 0 & 1 \end{bmatrix}}^{\text{Translate}} \cdot \overbrace{\begin{bmatrix} 1 & 0 & 0 & 0 \\ 0 & c_r & -s_r & 0 \\ 0 & s_r & c_r & 0 \\ 0 & 0 & 0 & 1 \end{bmatrix}}^{\text{Roll}} \cdot \overbrace{\begin{bmatrix} c_p & -s_p & 0 & 0 \\ s_p & c_p & 0 & 0 \\ 0 & 0 & 1 & 0 \\ 0 & 0 & 0 & 1 \end{bmatrix}}^{\text{Pitch}} \cdot \overbrace{\begin{bmatrix} c_y & 0 & -s_y & 0 \\ 0 & 1 & 0 & 0 \\ s_y & 0 & c_y & 0 \\ 0 & 0 & 0 & 1 \end{bmatrix}}^{\text{Yaw}}
$$

$$
\begin{bmatrix} 1 & 0 & 0 & t_x \\ 0 & 1 & 0 & t_y \\ 0 & 0 & 1 & t_z \\ 0 & 0 & 0 & 1 \end{bmatrix} \cdot \begin{bmatrix} 1 & 0 & 0 & 0 \\ 0 & c_r & -s_r & 0 \\ 0 & s_r & c_r & 0 \\ 0 & 0 & 0 & 1 \end{bmatrix} \cdot \begin{bmatrix} c_p c_y & -s_p & -c_p s_y & 0 \\ s_p c_y & c_p & -s_p s_y & 0 \\ s_y & 0 & c_y & 0 \\ 0 & 0 & 0 & 1 \end{bmatrix}
$$

$$
\begin{bmatrix} 1 & 0 & 0 & t_x \\ 0 & 1 & 0 & t_y \\ 0 & 0 & 1 & t_z \\ 0 & 0 & 0 & 1 \end{bmatrix} \cdot \begin{bmatrix} c_p c_y & -s_p & -c_p s_y & 0 \\ c_r s_p c_y - s_r s_y & c_r c_p & -c_r s_p s_y - s_r c_y & 0 \\ s_r s_p c_y + c_r s_y & s_r c_p & -s_r s_p s_y + c_r c_y & 0 \\ 0 & 0 & 0 & 1 \end{bmatrix}
$$

$$
\begin{bmatrix} c_p c_y & -s_p & -c_p s_y & t_x \\ c_r s_p c_y - s_r s_y & c_r c_p & -c_r s_p s_y - s_r c_y & t_y \\ s_r s_p c_y + c_r s_y & s_r c_p & -s_r s_p s_y + c_r c_y & t_z \\ 0 & 0 & 0 & 1 \end{bmatrix} = \mathrm{Q_{mat}}
$$

Symbol definitions used in these transformation matrices are given below.

t_x Camera x translation, *in inches* from model origin

t_y Camera y translation, *in inches* from model origin

t_z Camera z translation, *in inches* from model origin

r Model roll angle, $s_r = \sin(r), \quad c_r = \cos(r)$

p Model pitch angle

y Model yaw angle

Finally, the coefficients obtained from the field calculations were related to the inputs required by the model generation program by the following approximations.

$$\overbrace{\begin{bmatrix} \alpha t_x \\ \alpha t_y \\ \alpha c_\psi \\ \alpha s_\psi \\ \mathrm{P_1} \\ \mathrm{P_2} \end{bmatrix}}^{\text{Homogeneous Solution}} \Longrightarrow \overbrace{\begin{bmatrix} \mathrm{x} \\ \mathrm{y} \\ \mathrm{z} \\ r \\ p \\ y \end{bmatrix}}^{\text{Model Parameters}}$$

$$\alpha = \sqrt{(\alpha c_\psi)^2 + (\alpha s_\psi)^2}$$

$$\mathrm{z} = z\alpha \qquad \mathrm{d} = \frac{z w_\mathrm{x}}{f_\mathrm{x}}$$

$$\mathrm{x} = \mathrm{x}\alpha + \frac{\mathrm{d}}{\alpha^2}(\alpha c_\psi \alpha t_x + \alpha s_\psi \alpha t_y)$$

$$\mathrm{y} = \mathrm{y}\alpha - \frac{\mathrm{d}}{\alpha^2}(\alpha c_\psi \alpha t_y - \alpha s_\psi \alpha t_x)$$

$$\begin{bmatrix} \mathrm{p_1} \\ \mathrm{p_2} \end{bmatrix} = \begin{bmatrix} c_\psi & -s_\psi \\ s_\psi & c_\psi \end{bmatrix} \cdot \begin{bmatrix} \mathrm{P_1} \\ \mathrm{P_2} \end{bmatrix} \quad \text{Recall :} \quad \begin{aligned} \mathrm{p_1} &= \frac{-\alpha}{\mathrm{d}}(s_\kappa s_\gamma) & \mathrm{P_1} &= \frac{\alpha}{\mathrm{d}}[s_\psi(c_\kappa s_\gamma) - c_\psi(s_\kappa s_\gamma)] \\ \mathrm{p_2} &= \frac{\alpha}{\mathrm{d}}(c_\kappa s_\gamma) & \mathrm{P_2} &= \frac{\alpha}{\mathrm{d}}[s_\psi(s_\kappa s_\gamma) + c_\psi(c_\kappa s_\gamma)] \end{aligned}$$

$$\psi = \mathrm{Atan2}(\alpha s_\psi, \alpha c_\psi) \quad \kappa = \mathrm{Atan2}(-\mathrm{p_1}, \mathrm{p_2}) \quad \gamma = \mathrm{Asin}\left(\frac{\mathrm{d}}{\alpha}\sqrt{(\mathrm{p_1})^2 + (\mathrm{p_2})^2}\right)$$

$$\mathrm{Q}'_{(r,p,y)} = \overbrace{\begin{bmatrix} c_\kappa & s_\kappa & 0 \\ -s_\kappa & c_\kappa & 0 \\ 0 & 0 & 1 \end{bmatrix}}^{\text{Rotate } u'v' \rightarrow u,v} \cdot \overbrace{\begin{bmatrix} 1 & 0 & 0 \\ 0 & c_\gamma & -s_\gamma \\ 0 & s_\gamma & c_\gamma \end{bmatrix}}^{\text{Rotate Out of Plane}} \cdot \overbrace{\begin{bmatrix} c_\kappa & -s_\kappa & 0 \\ s_\kappa & c_\kappa & 0 \\ 0 & 0 & 1 \end{bmatrix}}^{\text{Rotate } u,v \rightarrow u',v'} \cdot \overbrace{\begin{bmatrix} c_\psi & -s_\psi & 0 \\ s_\psi & c_\psi & 0 \\ 0 & 0 & 1 \end{bmatrix}}^{\text{Rotate } x,y \rightarrow u,v} \cdot \mathrm{Q}_{(r,p,y)}$$

$$\mathrm{Q}_{(r,p,y)} = \begin{bmatrix} c_p c_y & -s_p & -c_p s_y \\ c_r s_p c_y - s_r s_y & c_r c_p & -c_r s_p s_y - s_r c_y \\ s_r s_p c_y + c_r s_y & s_r c_p & -s_r s_p s_y + c_r c_y \end{bmatrix}$$

$$p' = \mathrm{Asin}\,(s'_p) \qquad y' = \mathrm{Atan2}\,(c'_p s'_y, c'_p c'_y) \qquad r' = \mathrm{Atan2}\,(s'_r c'_p, c'_r c'_p)$$

This modeling of the transformation coefficients proved adequate for all in plane model movement. A demonstration of this was shown in the example sequence where translation (x,y), scaling (z), and pitch were simultaneously displaced from the image feature model. Initial closure to the feature position was very rapid in all four degrees of freedom, with the asymptotic approach partially explained by the potential field characteristics. The remaining two degrees of freedom for the out of image plane transformations were not correctly modeled. While this prevented coupling with the model generation program, it did not prevent the direct transformation of the wireframe image. The results of some tests allowing six degrees of freedom are shown in Figures 22 through 24. Only the yaw parameter was different between the wireframe model and image features in Figure 22. As the blue outline indicates, a reasonable transformation did occur for six degrees of freedom. Figure 23 suggests that simultaneous closure in six dimensions may be possible even under fairly large displacements. The exception to this is shown in Figure 24, where model placement was too remote to meet the proximity assumptions in the algorithm calculations. ERIM anticipates a final automatic algorithm will restrict the number of parameters initially varied to ensure stable closure. In particular, the sequence would be to first translate, then permit scaling and in plane rotations, and finally allow out of plane angular corrections only after the model and feature data are closely aligned.

10.0 SYSTEM ACCURACY

During the meetings held at Eglin Air Force Base on September 10 and 11, several design considerations were discussed. Of particular interest to an error analysis, the following item was noted in Attachment 2, Summary of Discussion.

> The desired system accuracy is two (2) inches in object space at a distance of 50 feet to the target with a one (1) inch focal length lens.

In order to responsibly assess the feasibility of this accuracy, ERIM initiated a small scale effort to determine the impact of various errors on system accuracy. Some of the items investigated are given below.

- Accuracy of film geometry, i.e., size and position of the sprocket holes.
- Consistency of film geometry, i.e., the amount of shrinkage or warping.
- Positional accuracy of the film during exposure.
- Positional accuracy of the film copying process.
- Positional accuracy of the film transport being used for digitization/review
- Scanning accuracy of the digitization process.

In addition to these items, consideration must be given to focal plane distortion from optics and the variability of digitization. Several of these errors were readily available from the manufacturers. Analysis of the accuracy values greatly influenced the selection of upgraded GADS equipment. The basic geometry and measurements for the film are given in Figures 25 and 26.

Applying the same accuracy requirements in object space for 16mm and 35mm film presents a problem since the algorithm is working in image space with pixels. Thus, one inch represents 4 pixels for 35mm film and 10 pixels for 16mm film. Either of these pixel distances may appear generous until other system conditions are considered. Using the pixel sizes given in Figures 25 and 26, the manufacturers' published film tolerances are given in the table below. Dimensions are given in pixels, 8.62μm per pixel for 16mm, 21.22μm per pixel for 35mm.

Film	Column	Line	Line (over 100 perfs)
16mm	3.48	1.51	92.81 (100 perfs = 100 frames)
35mm	2.37	2.45	17.91 (100 perfs = 25 frames)

The tolerance for 100 film perfs represents over 18 inches in object space for 16mm film, and just under 9 inches in object space for 25 frames of 35mm film. For analysis performed with film copies of the original, the minimum increase in tolerance would be additive, or a doubling of these figures. Add to this any positional errors from transport equipment (camera, copying, digitization) including adjustments for sprocket and mechanism wear, and an overall system accuracy assessment becomes very difficult to quantify.

For the purposes of assessing an automatic matching algorithm, overall accuracy considerations could be avoided by utilizing a standard set of digital imagery. Given that the true location of the target is not available, assessing automated performance probably entails a comparison with manual operations. One possible comparison would be of the operator and automated residuals from the fitted trajectory of the target. The automatic algorithm will minimize the aggregate distance of the extracted image features to the model data to obtain an optimal overall fit. ERIM anticipates this procedure will result in residuals with a smaller standard deviation and perhaps a small bias when compared with residuals from manual target placement.

As a final note on this subject, the sensitivity of the results in each of the six degrees of freedom needs to be considered. As an example of this, consider a wireframe model viewed directly "head-on." Changes in roll from this perspective should be resolvable to small angles. In contrast, small changes in pitch or yaw are unlikely to result in a change in the digitized representation of the model. Rendition errors will also arise in the potential field and when considering the features extracted from digital imagery. An analysis of errors must be able to accommodate all these sources.

11.0 SUMMARY AND RECOMMENDATIONS

An algorithm for automatically matching wireframe model data to edges extracted from digitized film images was designed and the critical portions were developed and demonstrated. The approach leverages existing hardware and software, interfacing with an operator via integration with manual operations. From an algorithmic perspective, ERIM would expect future work on automation of GADS model matching to address the following areas:

- Resolve the final 2-degrees of freedom
  - Separate parts with invariant shapes for an axis of rotation
  - Reformulate equations utilizing 8 coefficients
- Image feature extraction strategies (Algorithm step 2, edges)
  - Color based imagery
  - Edge linking or removal for regions of interest
  - Edge thinning, minimum continuity criteria
  - Integration with factors arising from potential field model
- Potential field generation
  - Continuous domain to discrete domain approximations
  - Region of stability (what's close enough?)
  - Correct correlation closure characteristics (rate, damping)
- Transformation determination (least squares)
  - Sensitivity to extraneous or incorrect image features
  - Treatment of aligned versus non-aligned model pixels
  - Weighting of images features
- Error analysis
  - Covariance of errors (model parameters)
  - Quantization errors (edge accuracy, model rendition, field rendition)
  - Determine system accuracy (film, camera, transport, digitization, ...)

While several challenging areas remain for development, the results of this feasibility study indicate an automated upgrade to manual GADS is achievable. The development of this capability would also enhance manual efforts for model matching through the quantitative feedback of model fit and error analysis results. Given this approach to automated GADS is possible and well integrated with existing capability, further development appears appropriate and is encouraged.

Appendix A

LITERATURE SURVEY

ERIM performed a literature search using the computer based Dialog Information Retrieval Service. A description of the four database files queried is given below.

NTIS Produced by the National Technical Information Service of the U.S. Department of Commerce, the central source for the public sale and dissemination of U.S. government–sponsored research, the database represents reports from the U.S. Department of Energy (DOE), U.S. Department of Defense (DOD), National Aeronautics and Space Administration (NASA), in addition to several other agencies.

INSPEC The Information Services for Physics, Electronics, and Computing is the largest English–language database for the fields of physics, electrical engineering, electronics, computers, control engineering, and information technology. It scans over 3,900 journals and serials, and includes source material from conference proceedings and papers (approximately 20%), books, dissertations, and reports.

SPIN The Searchable Physics Information Notices covers all major areas of physics. References are drawn from all English–language and Russian journal articles and conference proceedings published by the AIP and its member societies along with other select American journals.

SUPERTECH This database consists of five subfiles with information related to the fields of biotechnology, artificial intelligence, CAD/CAM, robotics, and telecommunications. References are from over 9,000 worldwide sources including trade, scientific, legal, and policy journals; professional and technological conferences and symposia; university monographs; U.S. and international government agency reports and white papers, and independent laboratory studies.

Using a keyword search, the following number of titles were obtained from each file after initially reducing to only those entries that matched the keyword image()process?. Note that keyword usage of "()" prohibits matches with intervening words, while the "?" gives a match for any word ending.

Keyword	NTIS	INSPEC	SPIN	SUPERTECH
registration	159	90	3	15
feature()detect?	7	9	1	15
image()sequence()analysis	1	6	0	1
time()varying()imag?	15	23	0	9

For the two instances where more than 25 entries matched both keywords, only the first 25 were printed and examined. After this initial query, a second search was initiated with the following keywords and results:

Keyword	NTIS	INSPEC
image()sequence()analysis	1	17
time()varying()imag?	17	85
motion & image()sequence	6	96
moving()objects & image()sequence	3	17

Once again, only the first 25 entries were reviewed for matches with over 25 titles. A partial list of titles obtained from these searches and other efforts is given below.

"3-D Motion Estimation from Projections," SPIE Applications of Digital Image Processing IX (1986)

"A Temporal Edge-Based Image Segmentor," Pattern Recognition, Vol. 20, No. 3, 1987

"Adaptive Gray Scale Mapping to Reduce Registration Noise in Difference Images," Computer Vision, Graphics, and Image Processing, **33** (1986)

"An Adaptative Image Sequence Filtering Scheme Based on Motion Detection," SPIE Architectures and Algorithms for Digital Image Processing (1985)

"Application of the One-Dimensional Fourier Transform for Tracking Moving Objects in Noisy Environments," Computer Vision, Graphics, and Image Processing **21** (1983)

"Correlation of Adjacent Pixels for Multiple Image Registration," IEEE Transactions on Computers (7/85)

"Extracton of Motion Data by Interactive Image Processing," IEEE CH1318 (5/78)

"Detection of Moving Objects Using Line Image Sequence," IEEE CH2046 (1/84)

"Dynamic Imagery Analysis via Distributed Parameter Systems: Characteristics, Discontinuities, Weak Solutions and Shocks," IEEE CH1761 (6/82)

"Man-Made Objects Dynamic Recognition Using Gray Levels Corners," SPIE Architectures and Algorithms for Digital Image Processing (1985)

"Motion Modeling and Prediction," IEEE CH2342 (4/86)

"Parameter Space Techniques for Image Registration," Proceedings of IGARSS 1986 Symposium

"Recursive Image Registration with Application to Motion Estimation," IEEE Transactions on Acoustics, Speech and Signal Processing (1/87)

"Registration and Rectification of Images Using Image Algebra," IEEE CH2398 (6/87)

"Residual Recursive Displacement Estimation," IEEE CH1595 (8/81)

"Robust Estimation of Three-Dimensional Motion Parameters from a Sequence of Image Frames Using Regularization," IEEE PAMI (7/86)

"Three-Dimensional Motion Analysis using Shape Change Information," SPIE Applications of Artificial Intelligence III (1986)

"Unique Recovery of Motion and Optic Flow via Lie Algebras"

"Visual Disparity as a Cue for Depth and Velocity in Real World Scenes," IEEE CH1318 (5/78)

Additional literature from various manufacturers also proved helpful when studying system accuracy issues. ERIM will be pleased to provide copies of these papers as requested by Eglin personnel.

Appendix B

FIGURES

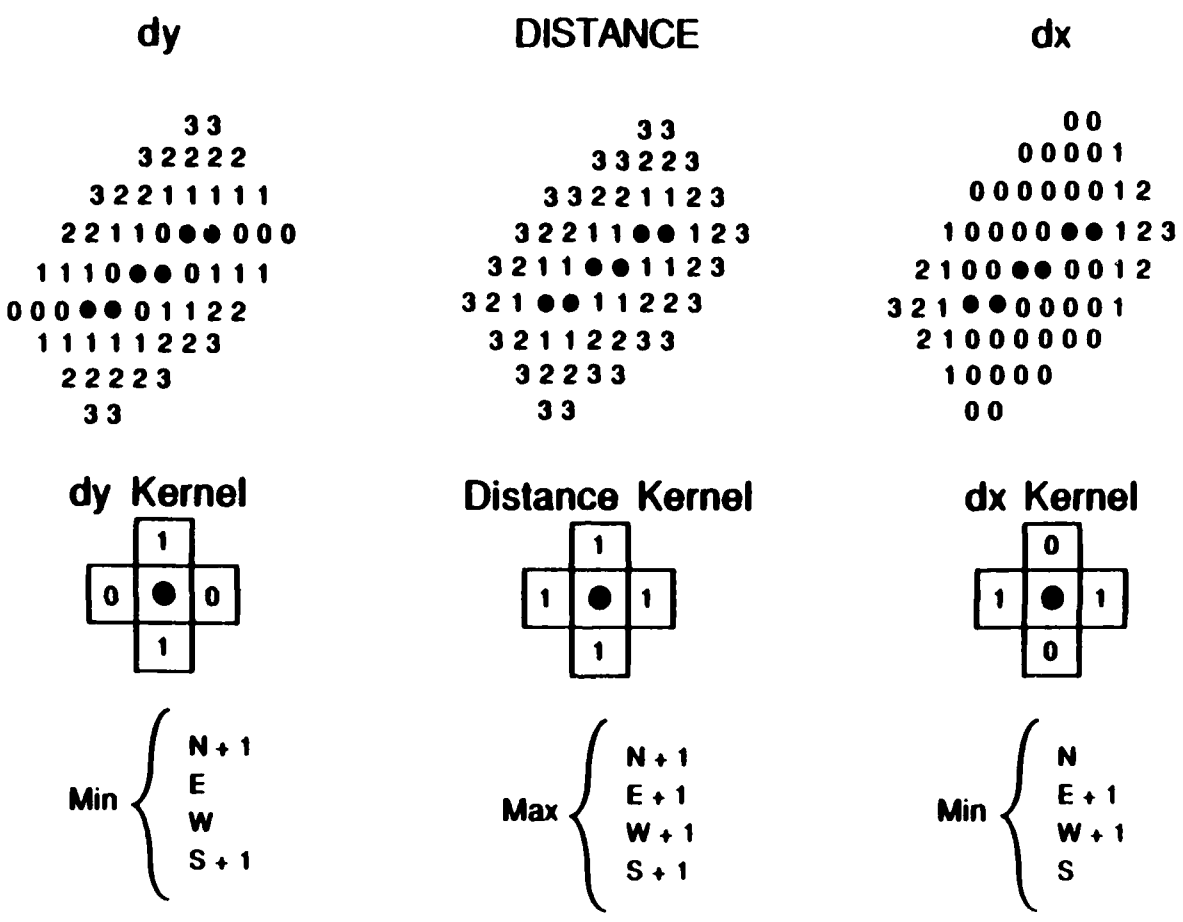

Figure 1: Potential Field Calculation

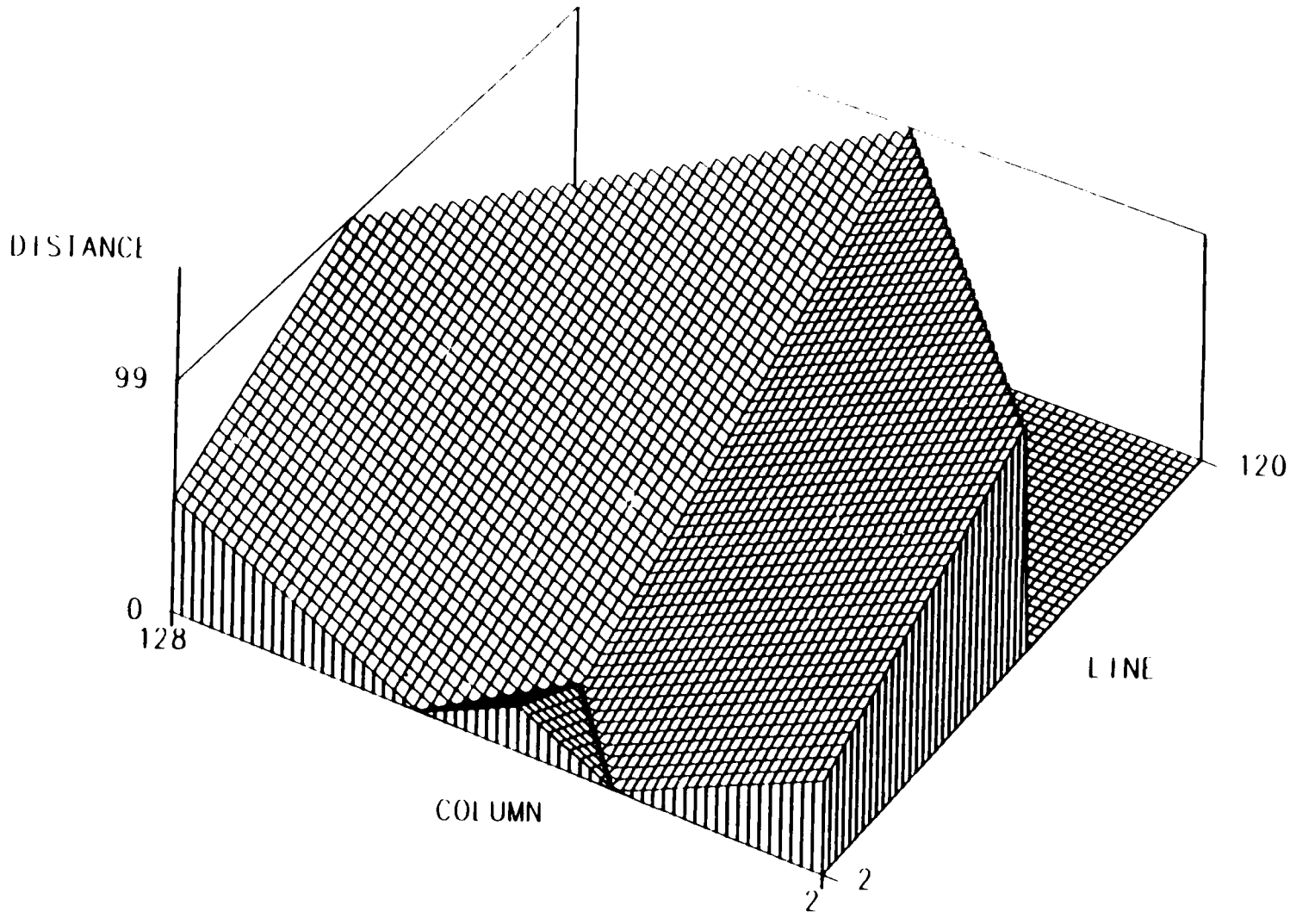

Figure 2: Potential Field Perspective Plot

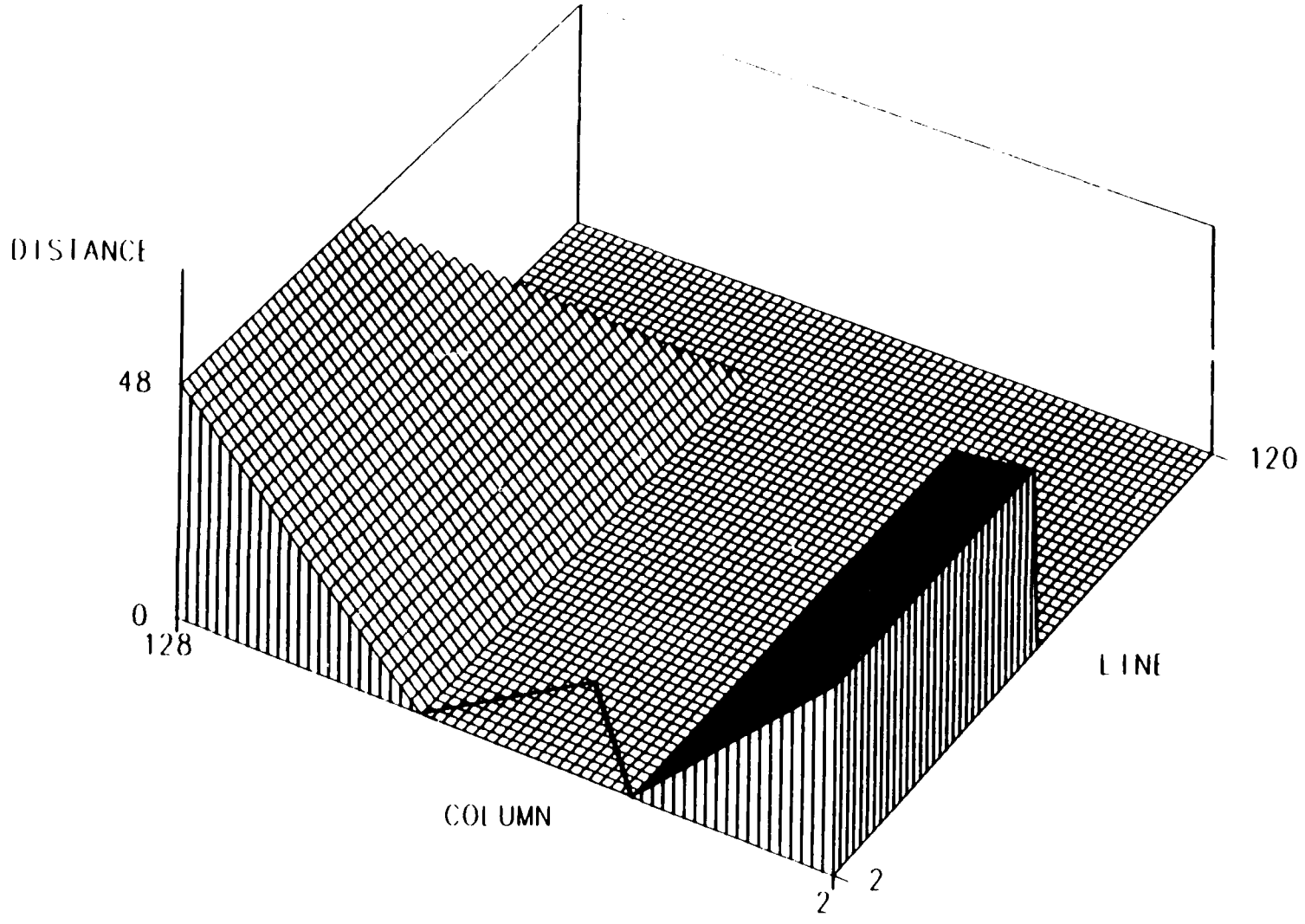

Figure 3: Potential Field Horizontal Component

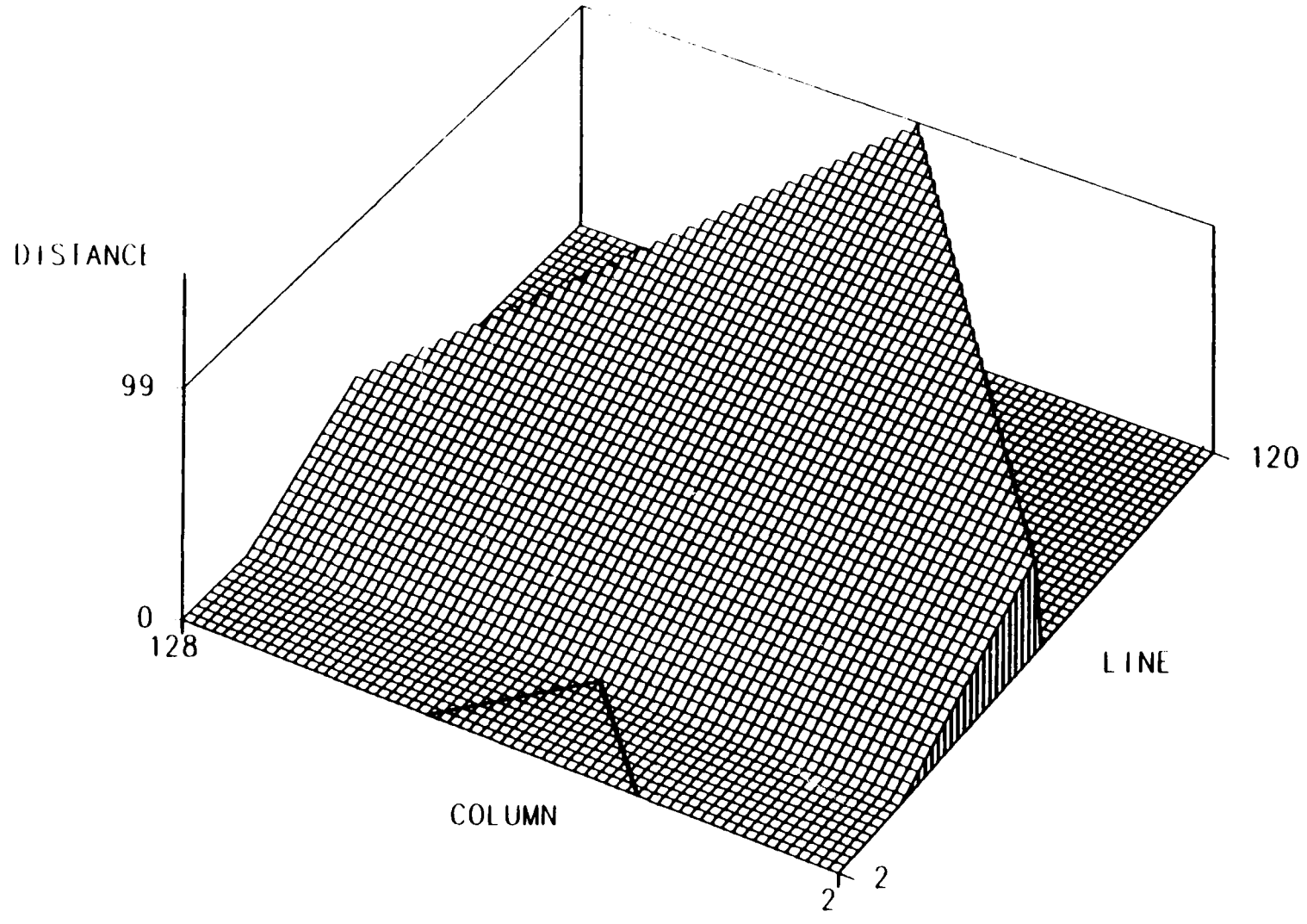

Figure 4: Potential Field Vertical Component

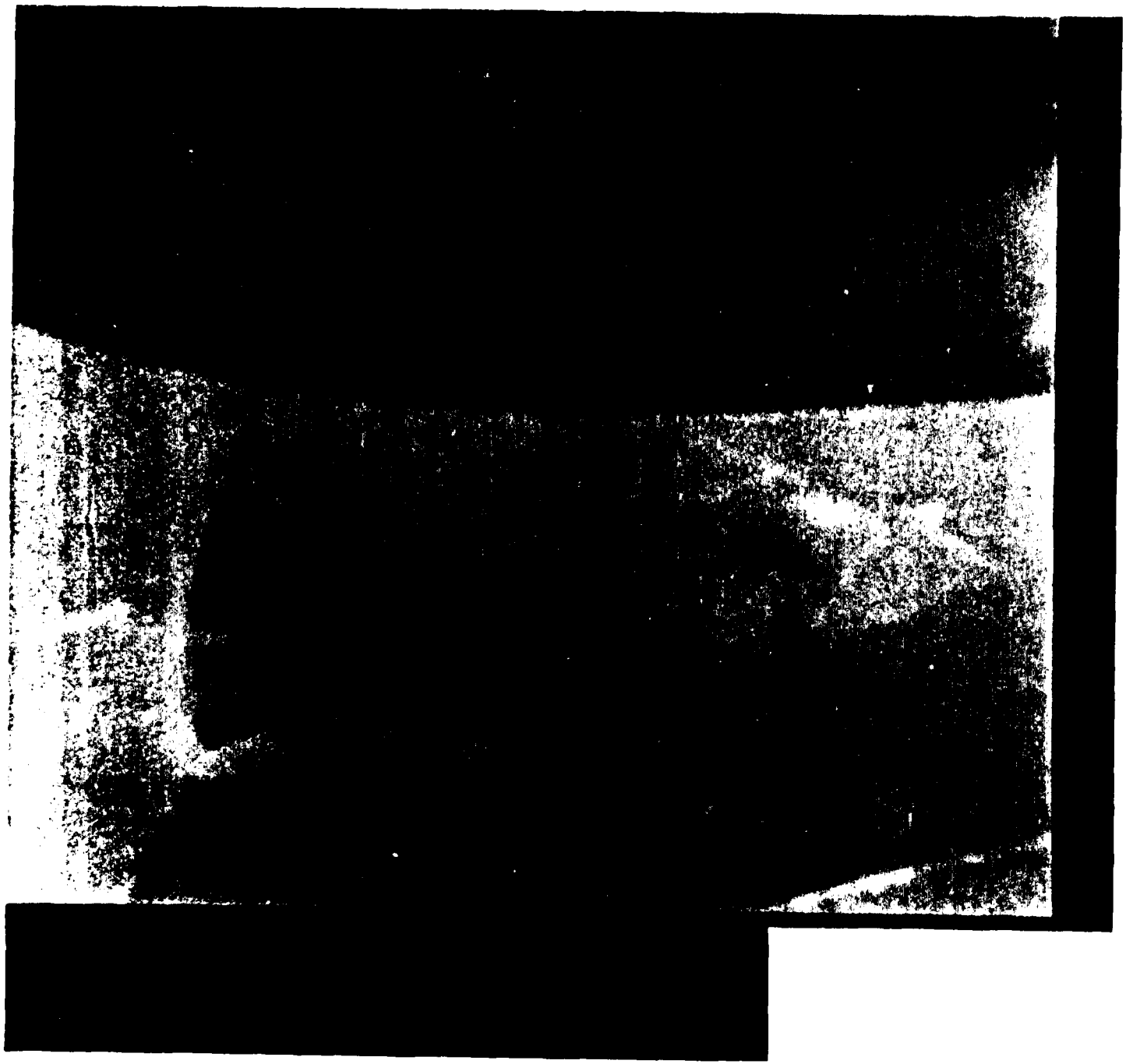

Figure 5. Example Image Frame

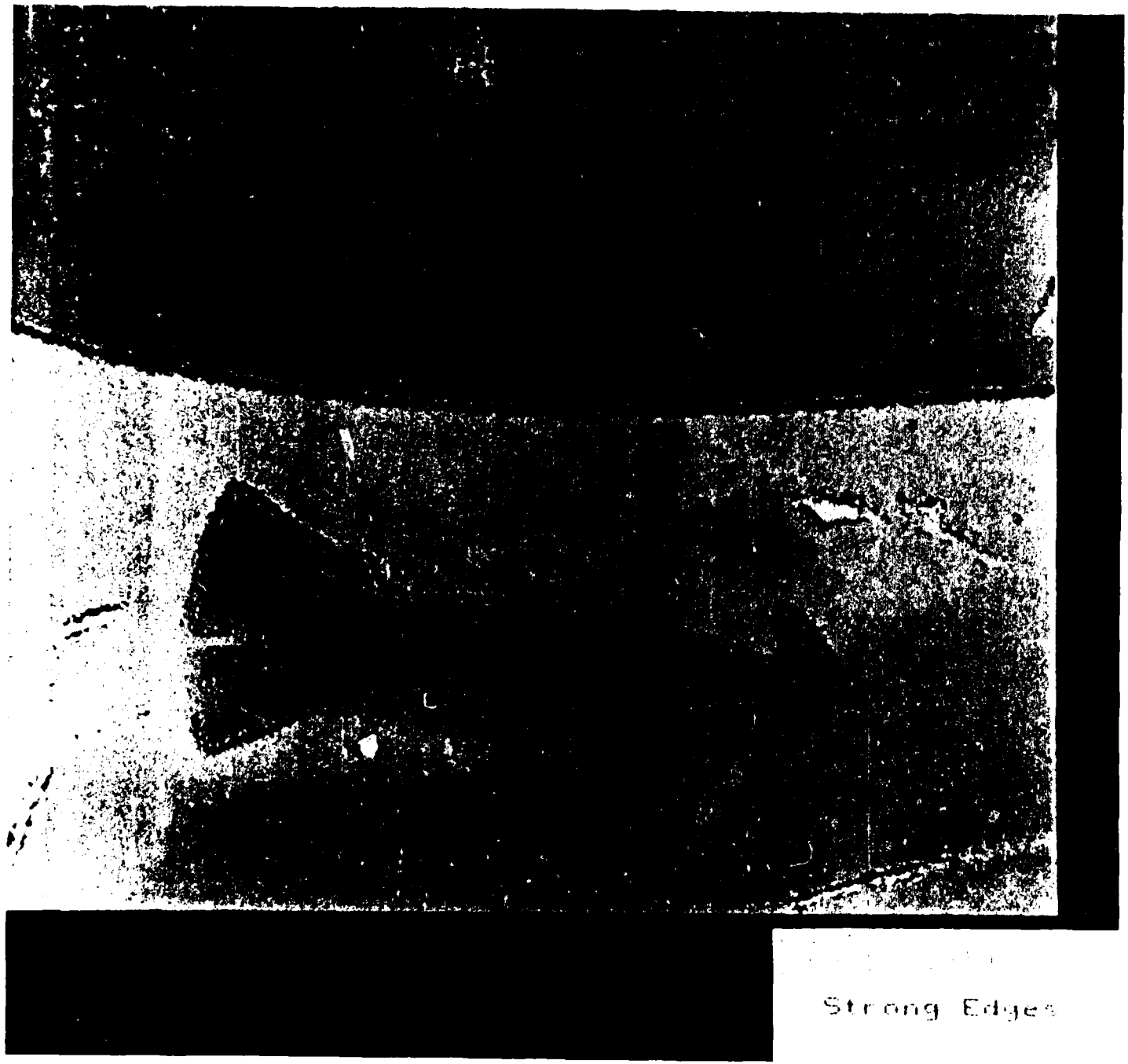

Figure 6. Image Feature Determination

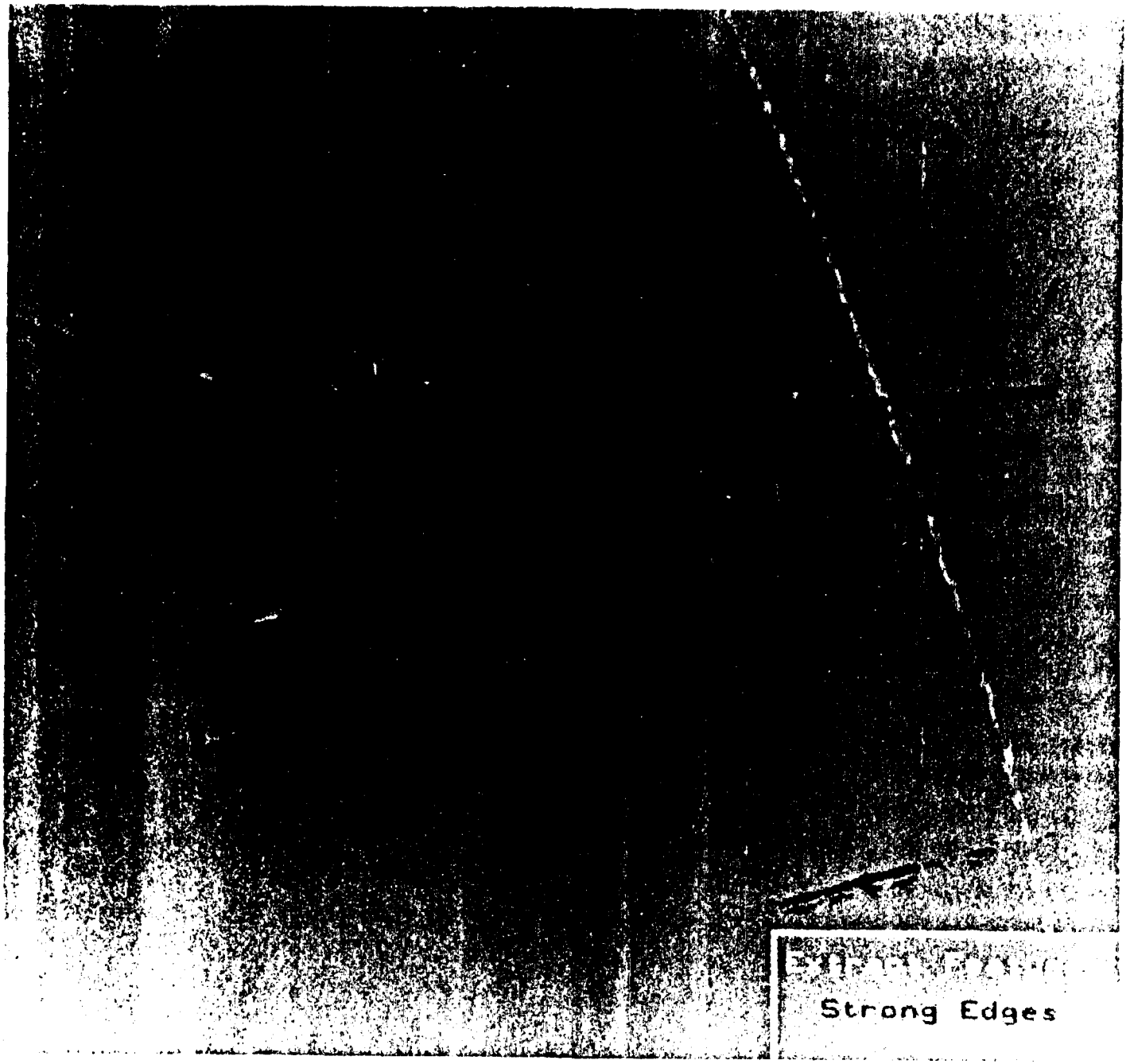

Figure 7. Image Feature Extraction

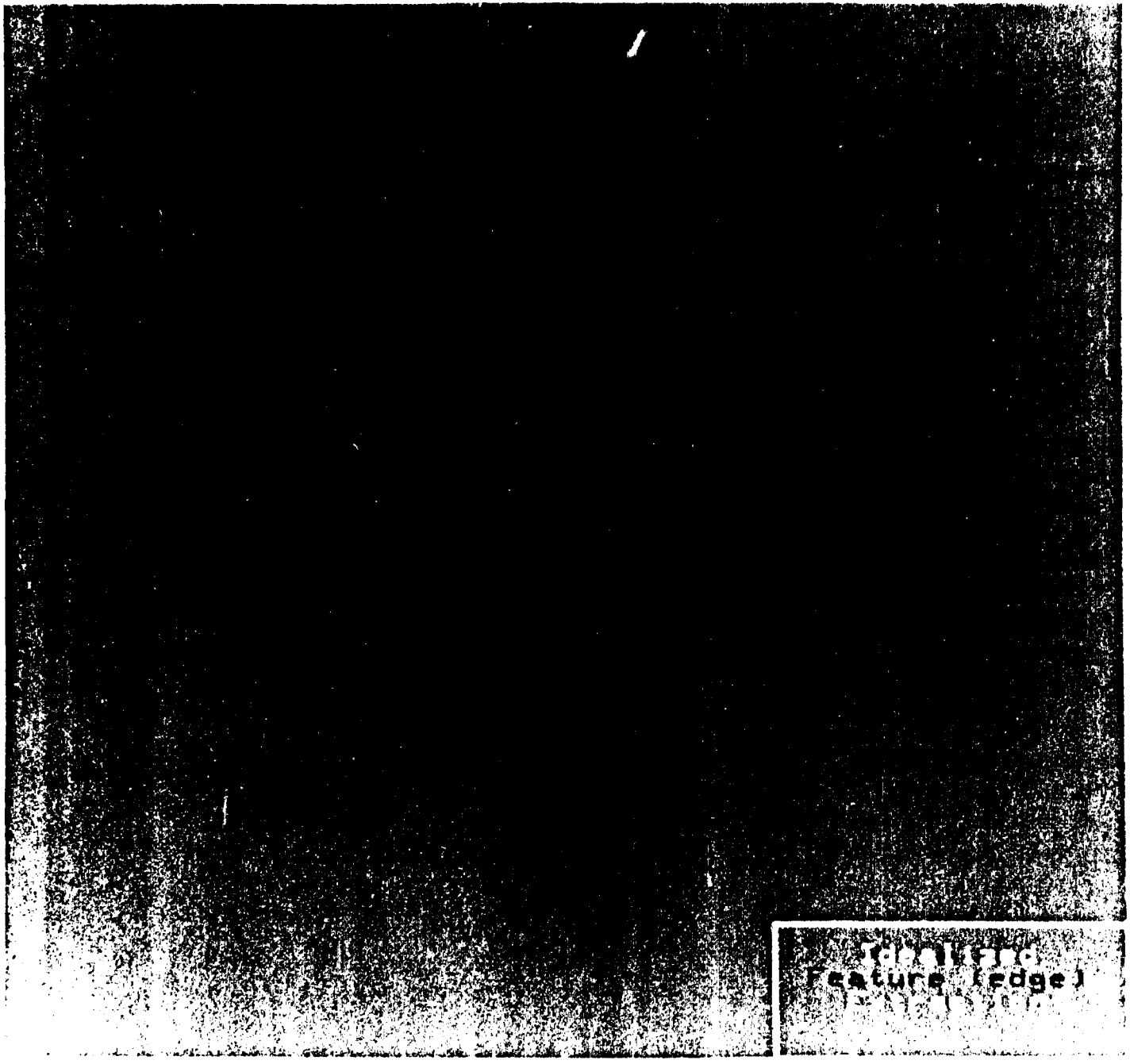

Figure 8. Idealized Feature Extraction

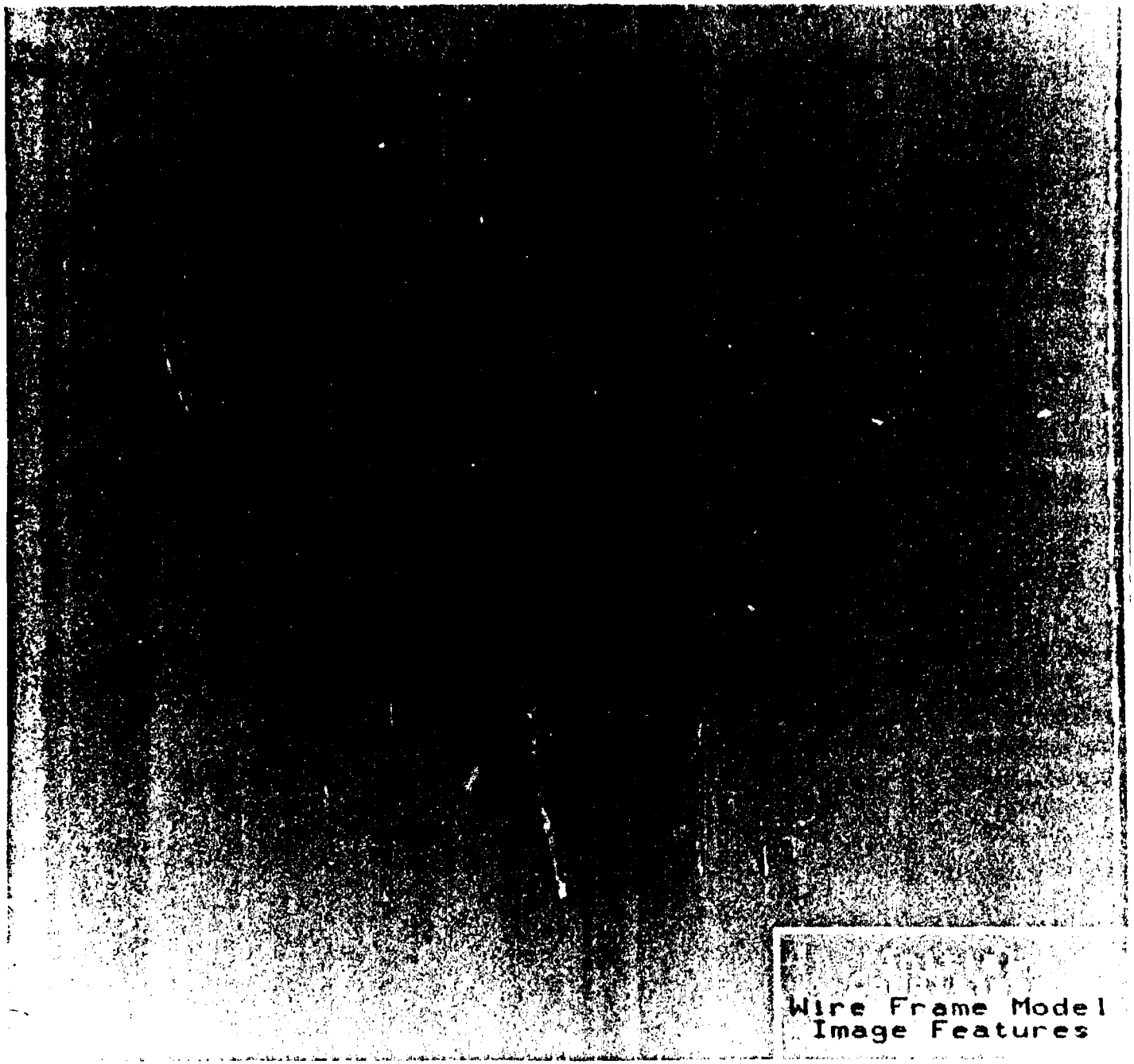

Figure 9. Initial Model Matching Conditions

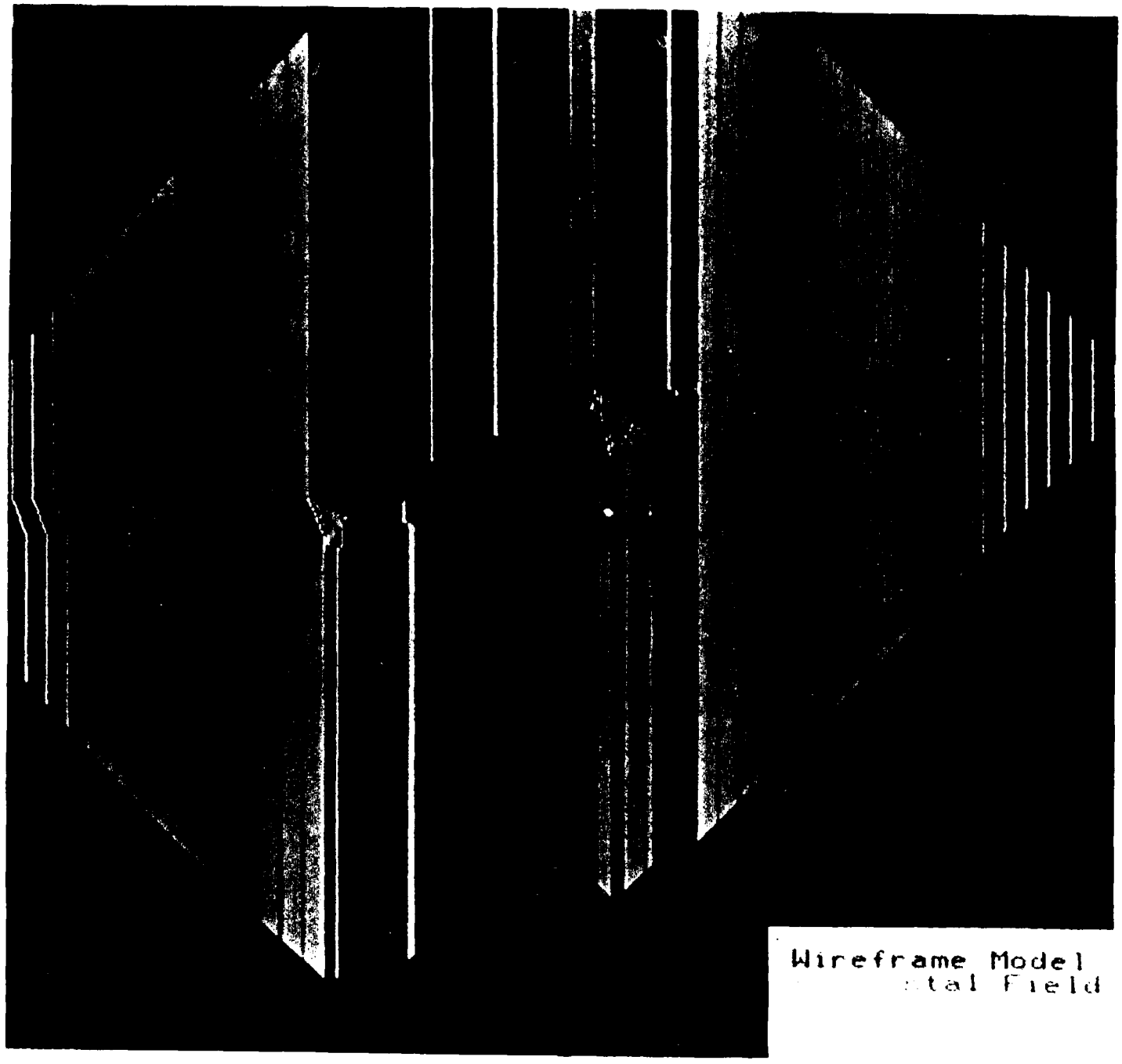

Figure 10. Horizontal Field for Wireframe Model

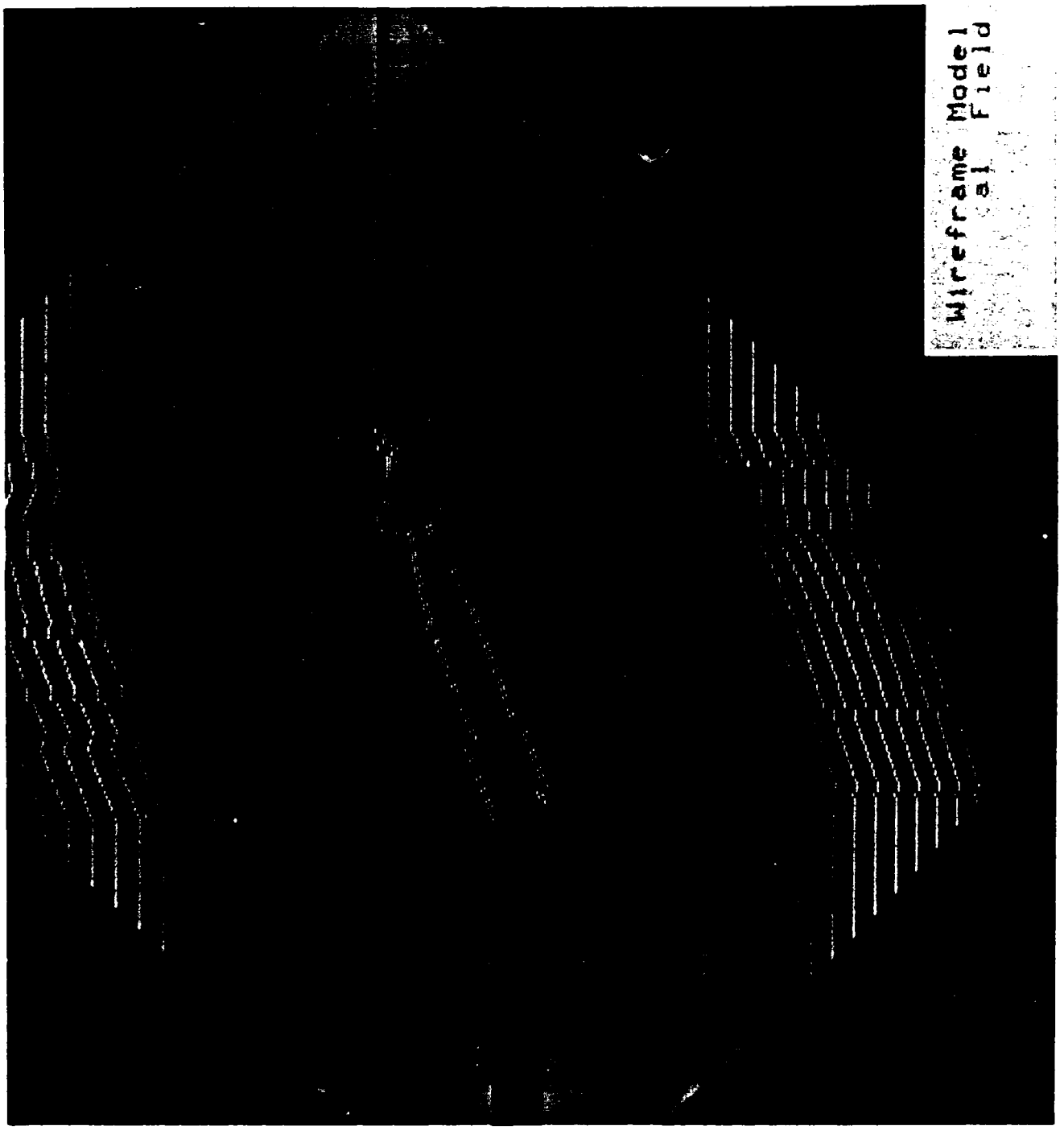

Figure 11. Vertical Field for Wireframe Model

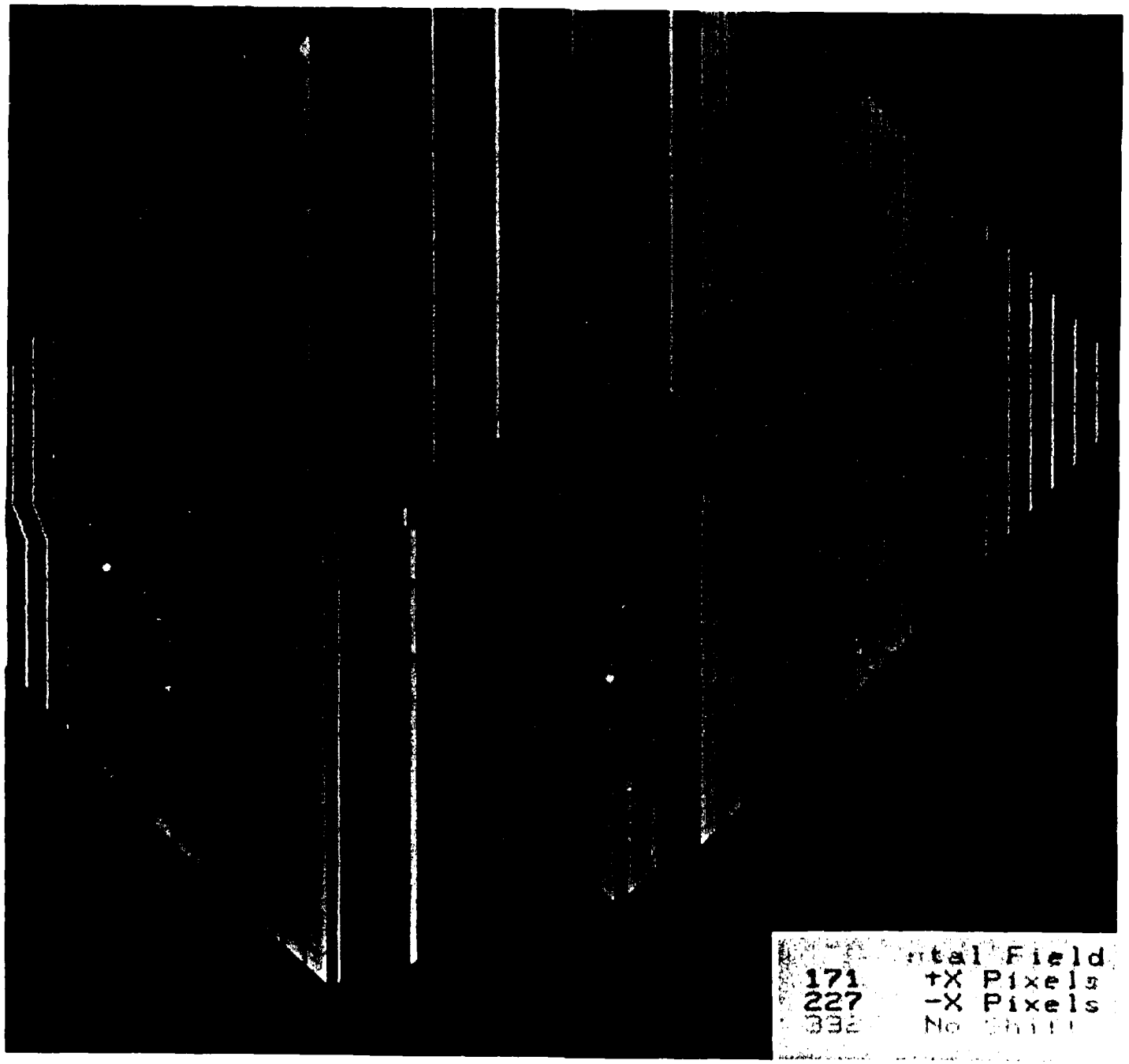

Figure 12. Loop 1, Idealized Features in Horizontal Field

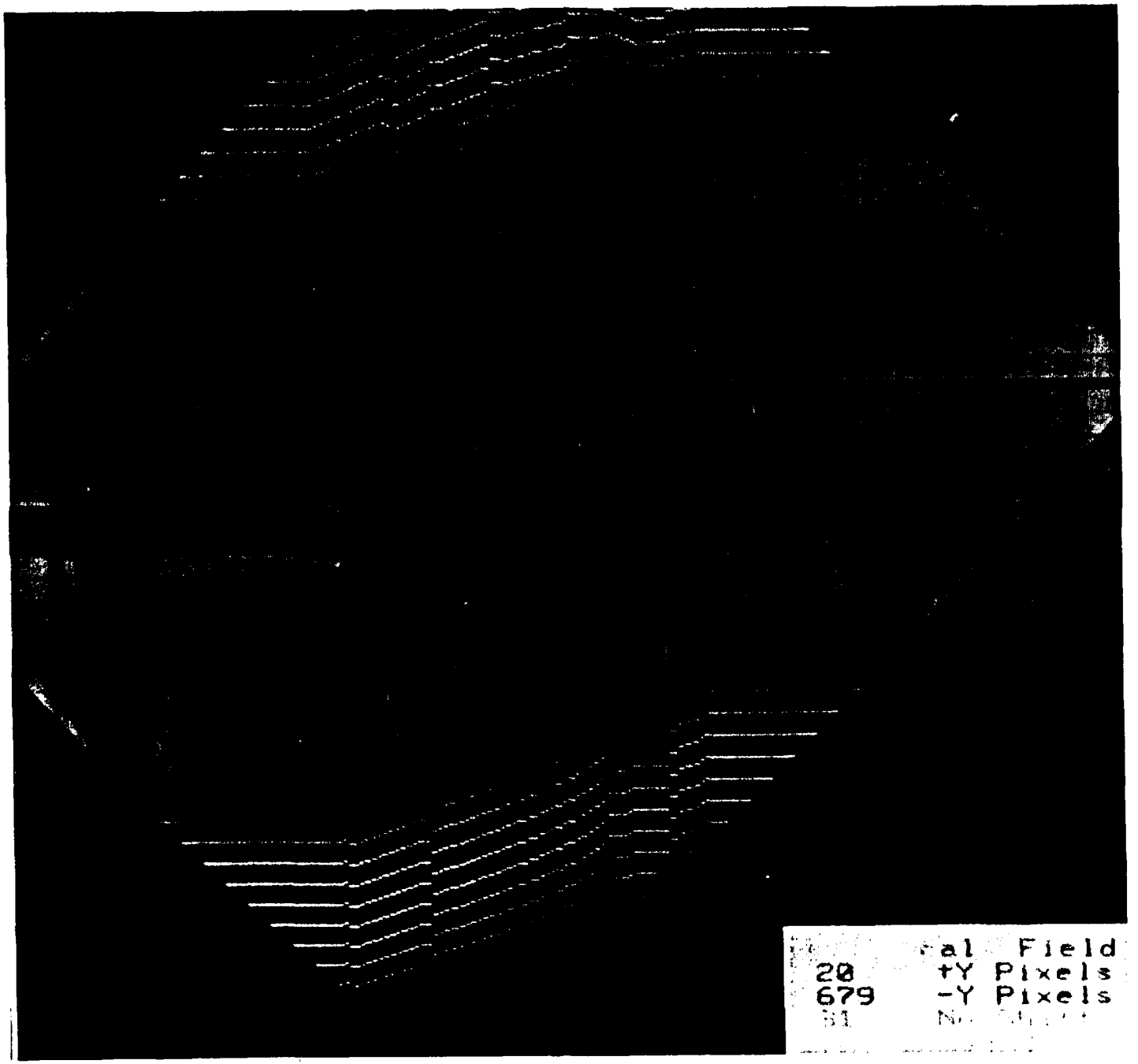

Figure 13. Loop 1, Idealized Features in Vertical Field

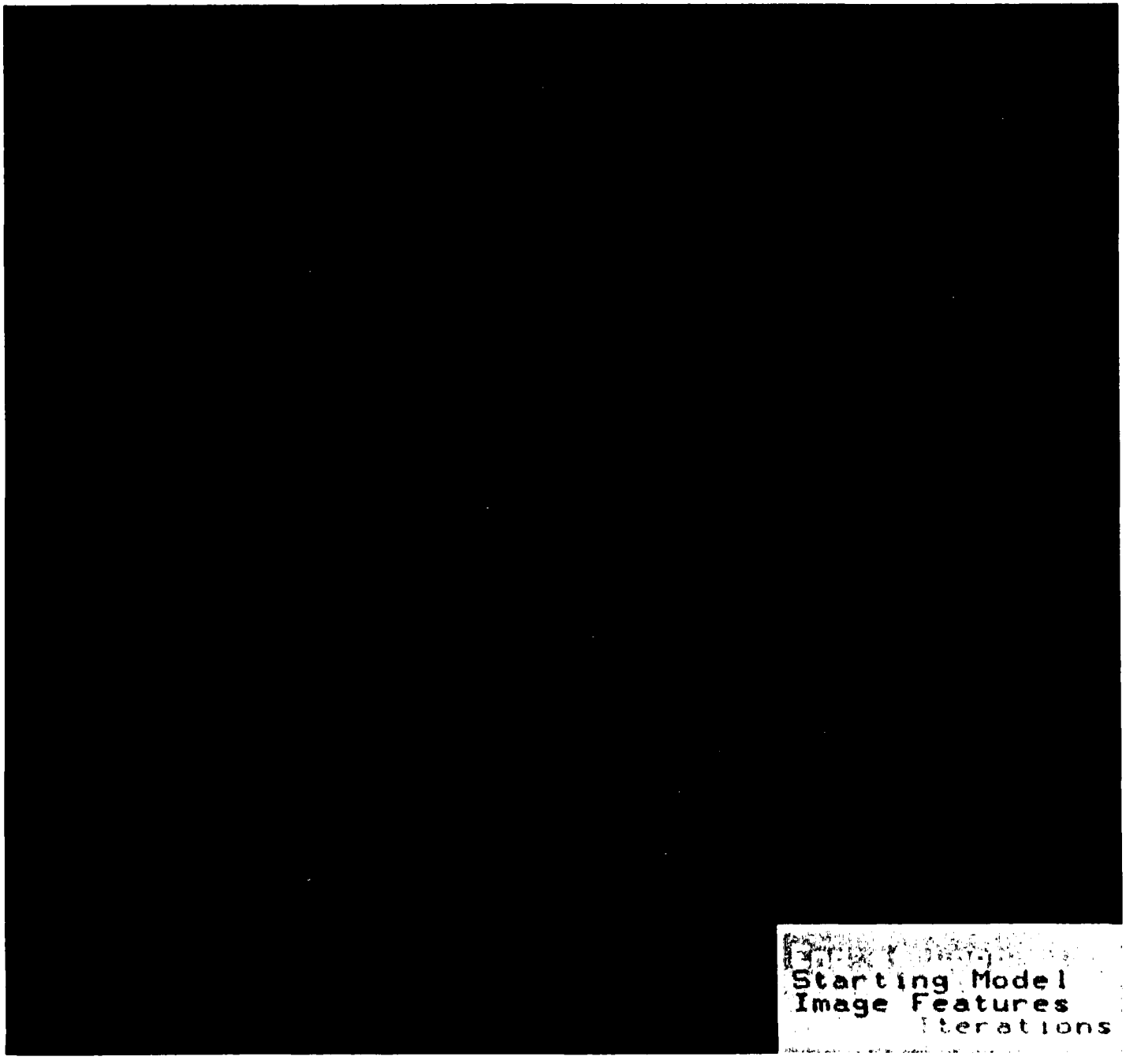

Figure 14. Loop 1, Model Relocation

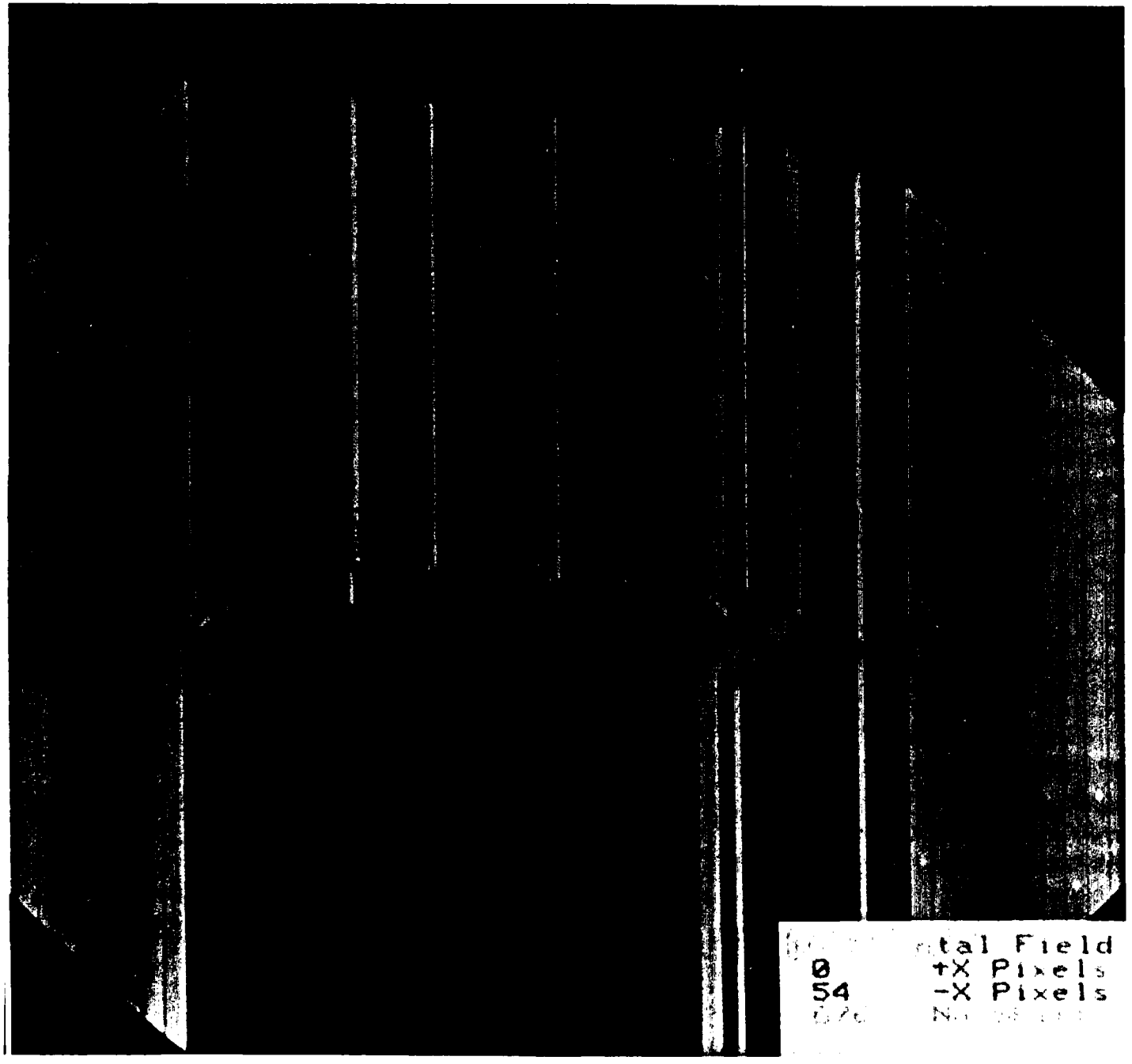

Figure 15. Loop 20, Idealized Features in Horizontal Field

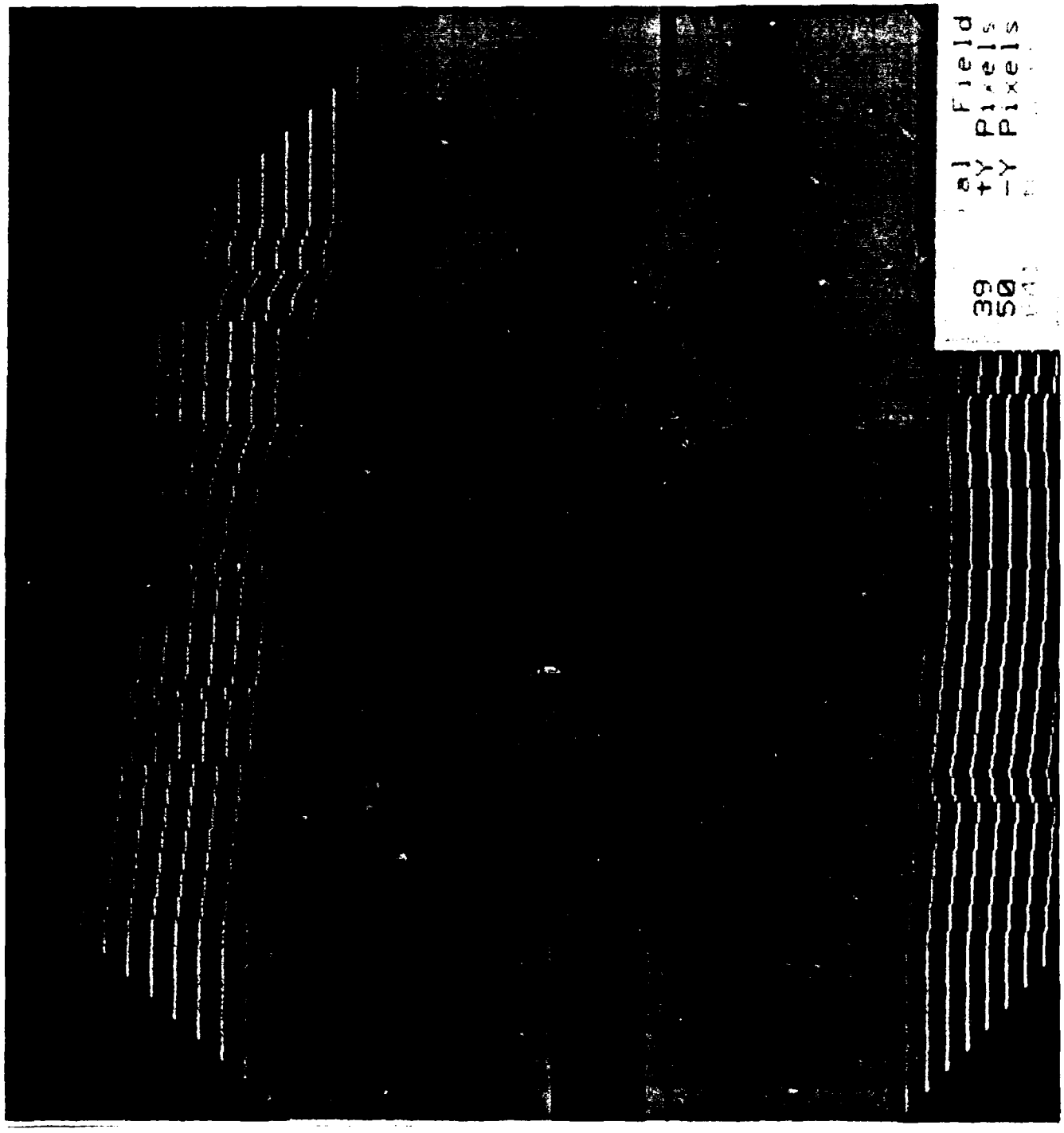

Figure 16. Loop 20, Idealized Features in Vertical Field

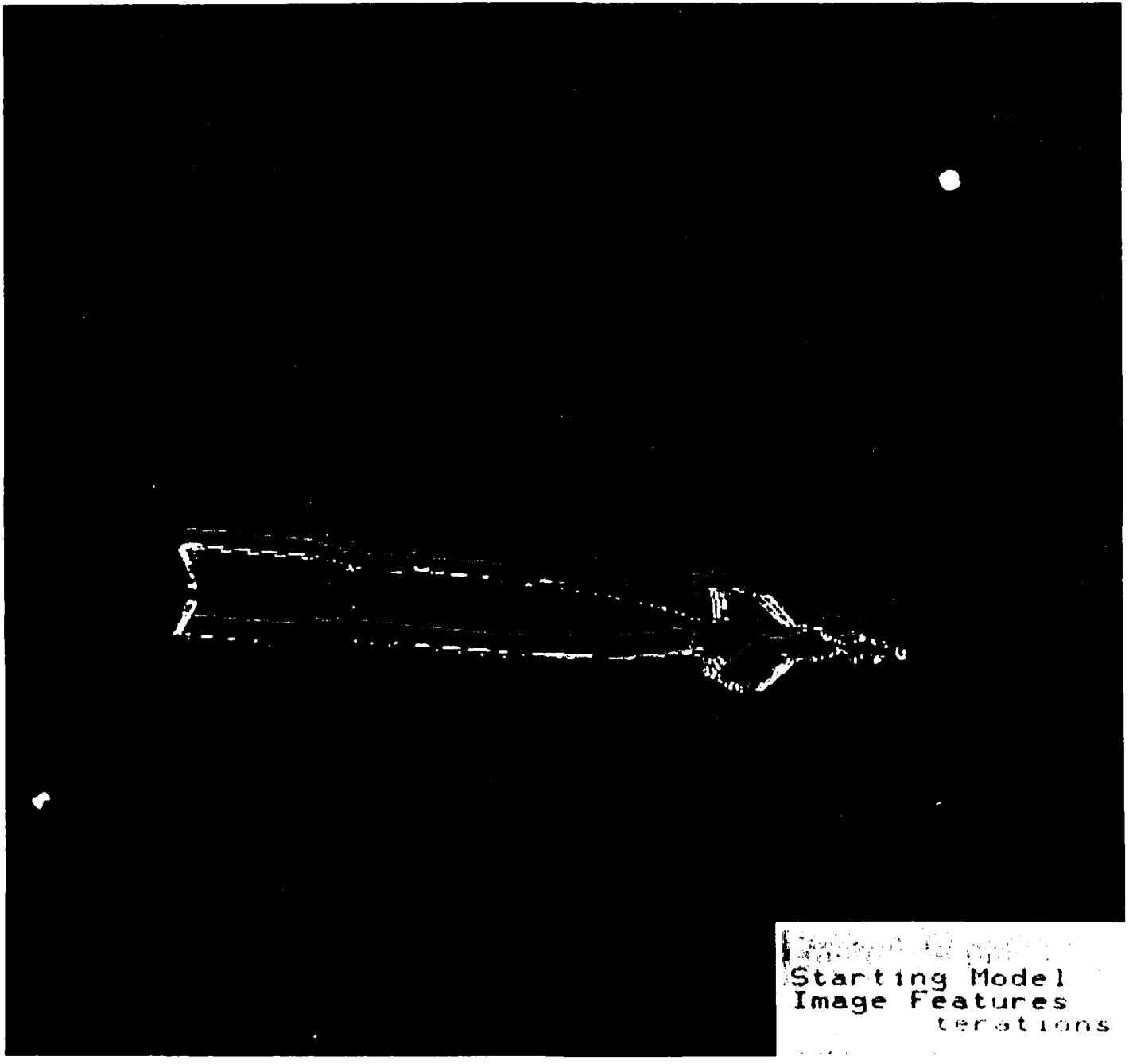

Figure 17. Loop 20, Model Relocation

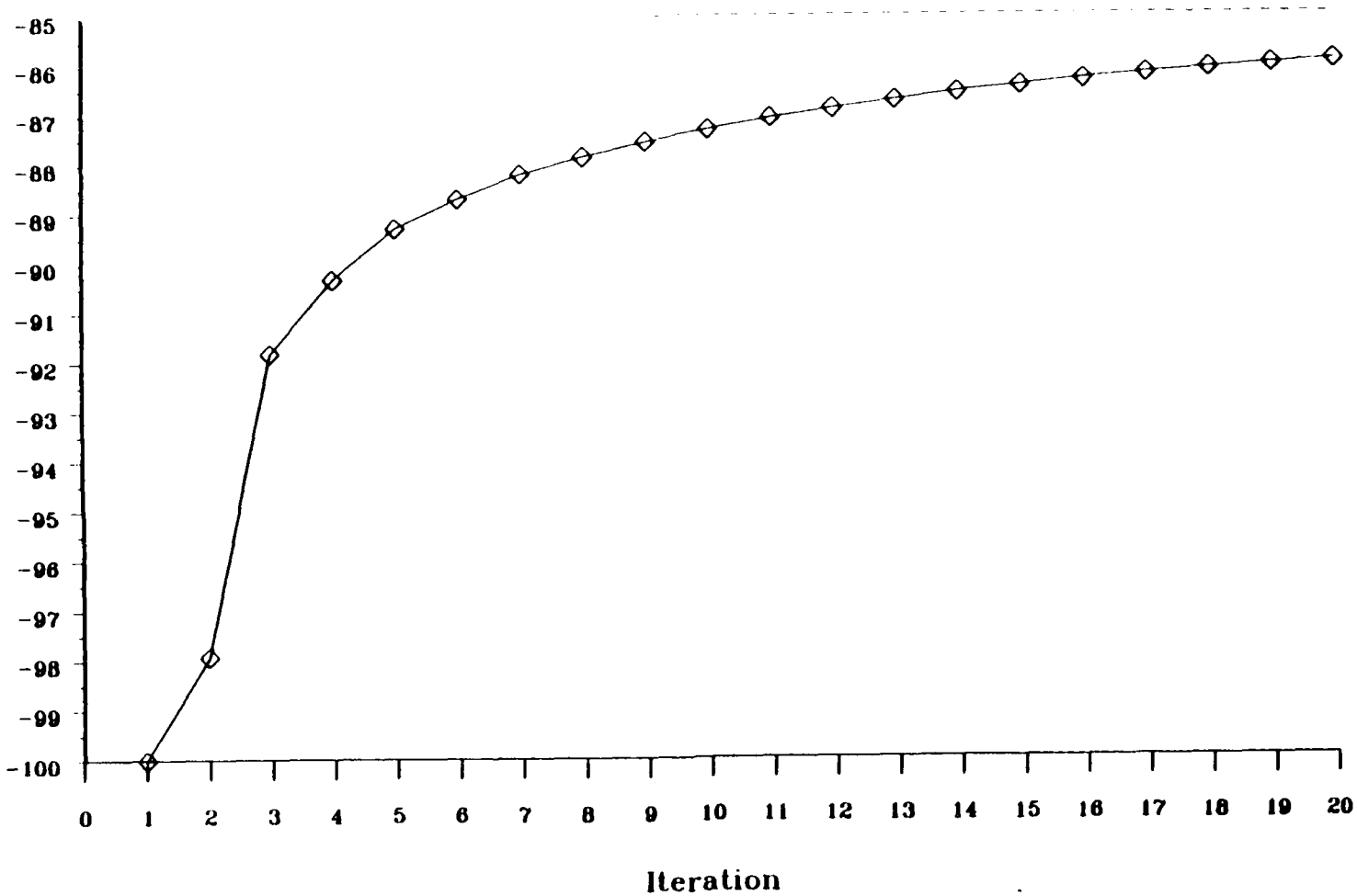

Figure 18: Closure of Model to Features, X Parameter

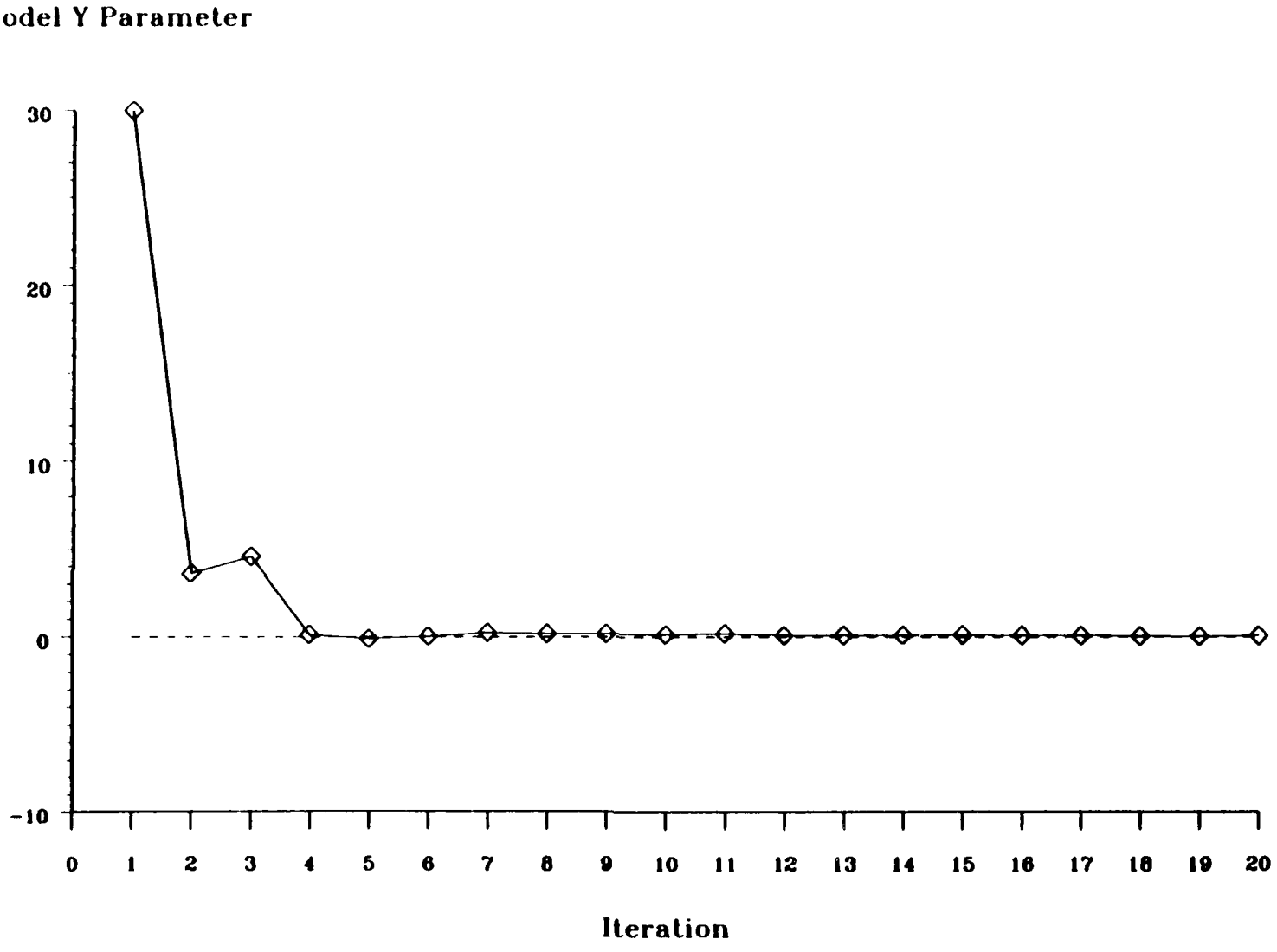

Figure 19: Closure of Model to Features, Y Parameter

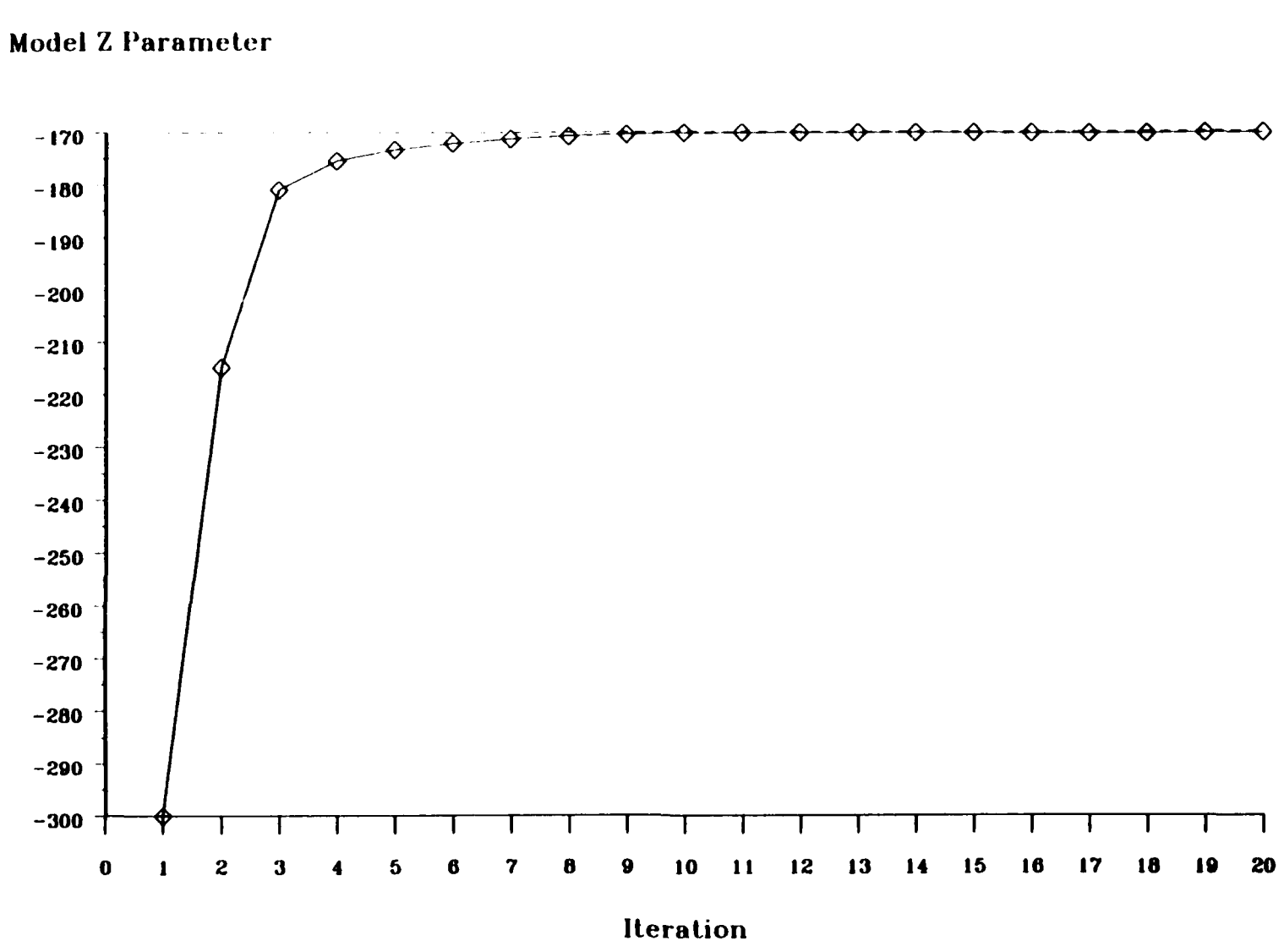

Figure 20: Closure of Model to Features, Z Parameter

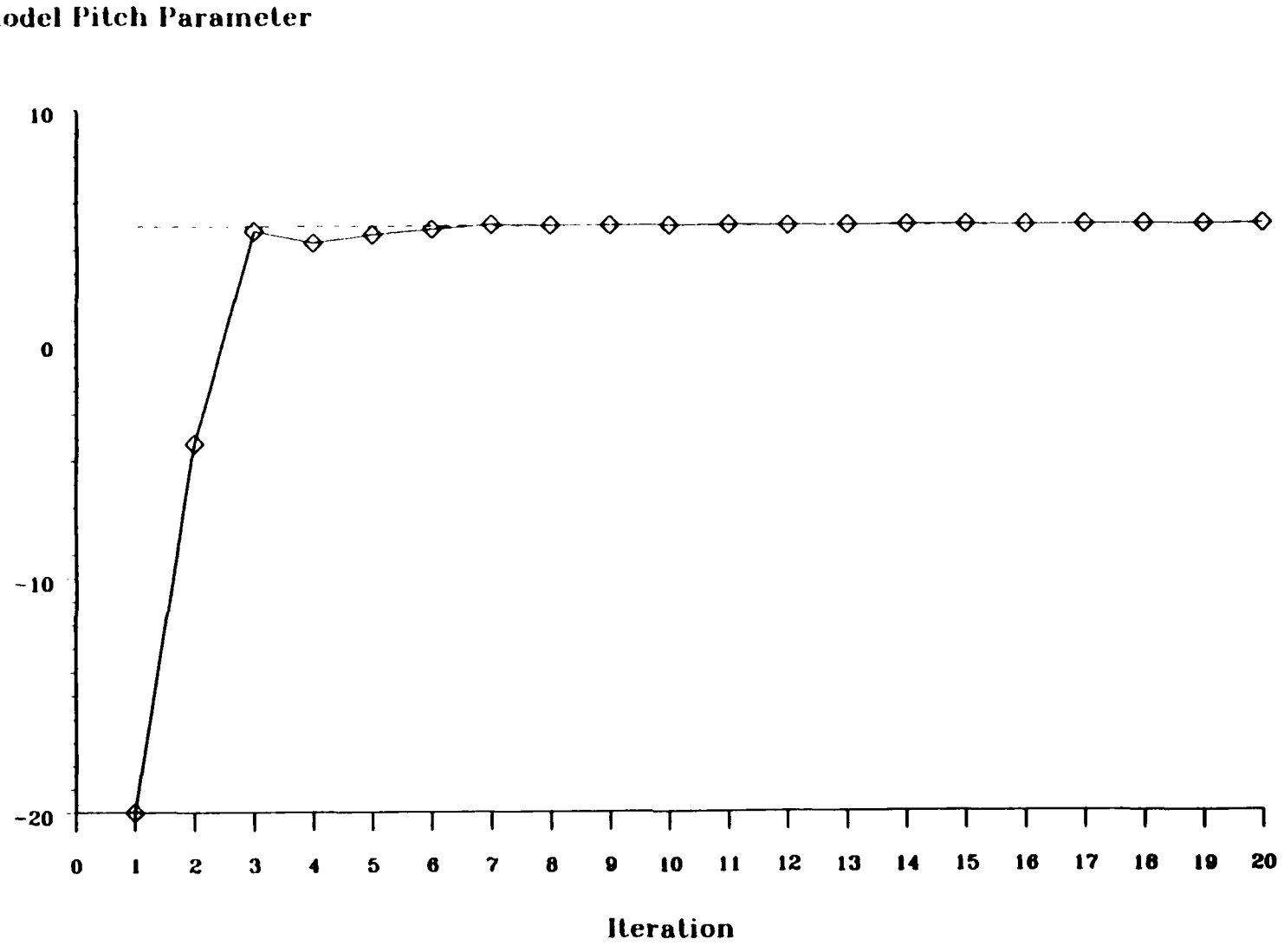

Figure 21: Closure of Model to Features, Pitch Parameter

Figure 22. Yaw Perturbation, Six Degrees of Freedom

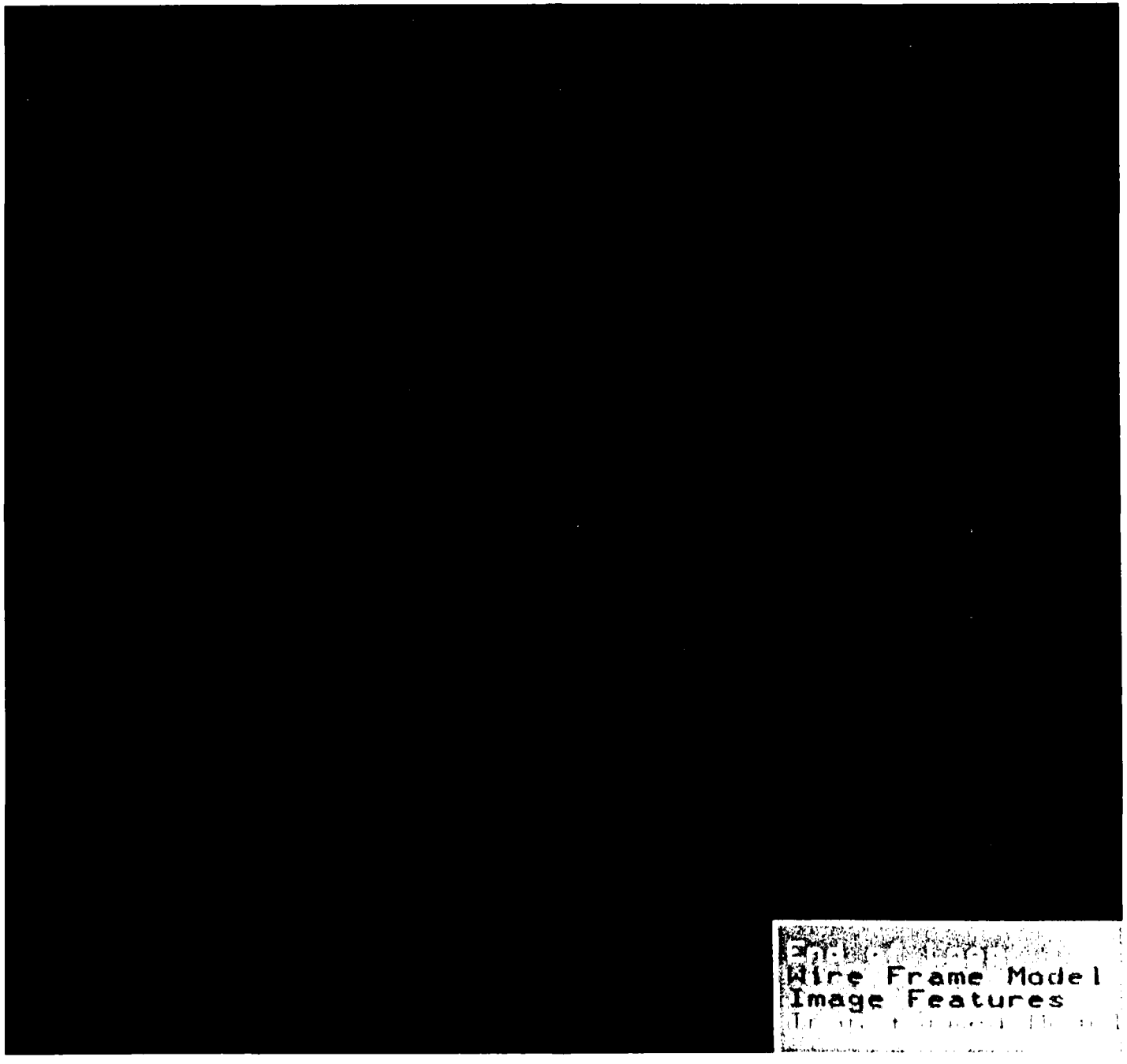

Figure 23. Perturbation in X, Z, Roll, Pitch, Yaw

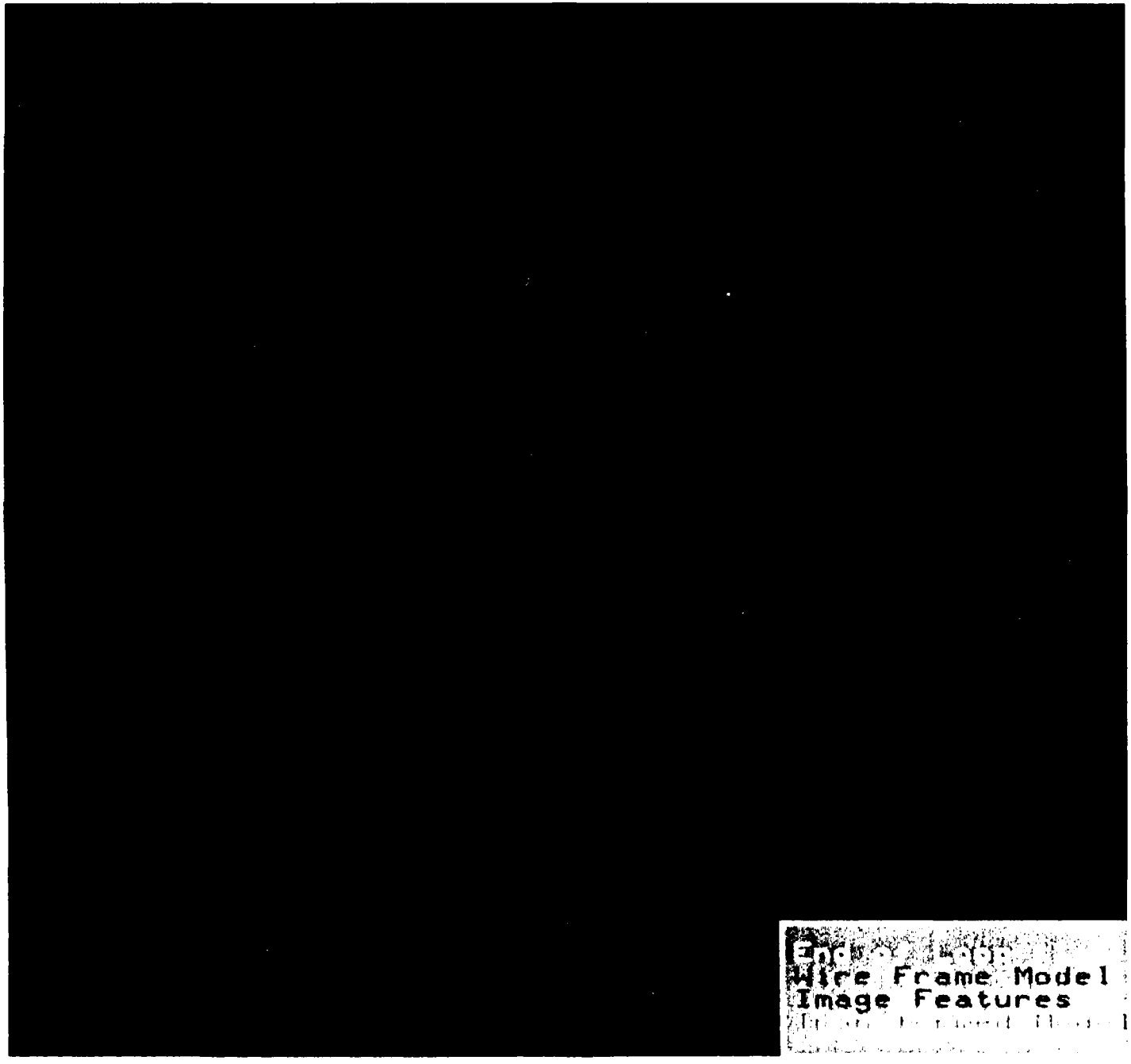

Figure 24. Perturbation Beyond Stable Response

EGLIN GADS - SYSTEM ACCURACY

GOAL: 2" in object space at a distance of 50' with a 1" focal length lens

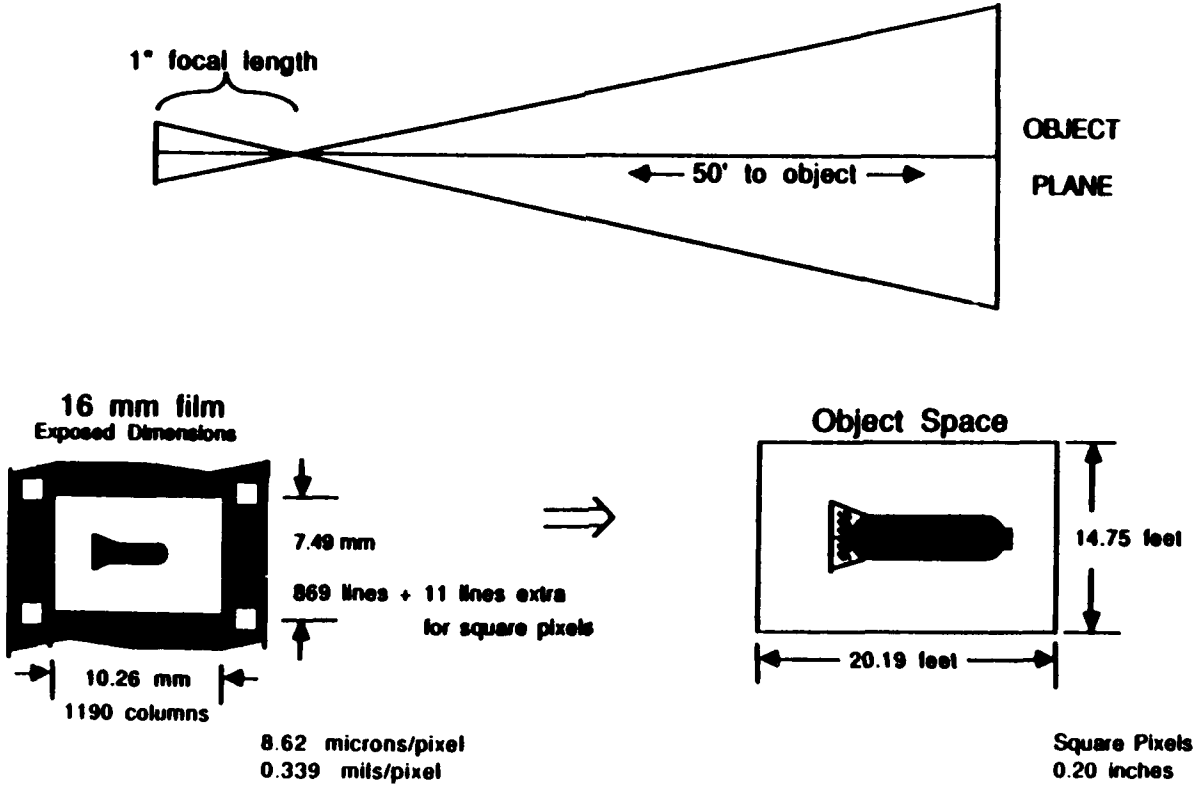

Figure 25: Geometry for 16mm Film

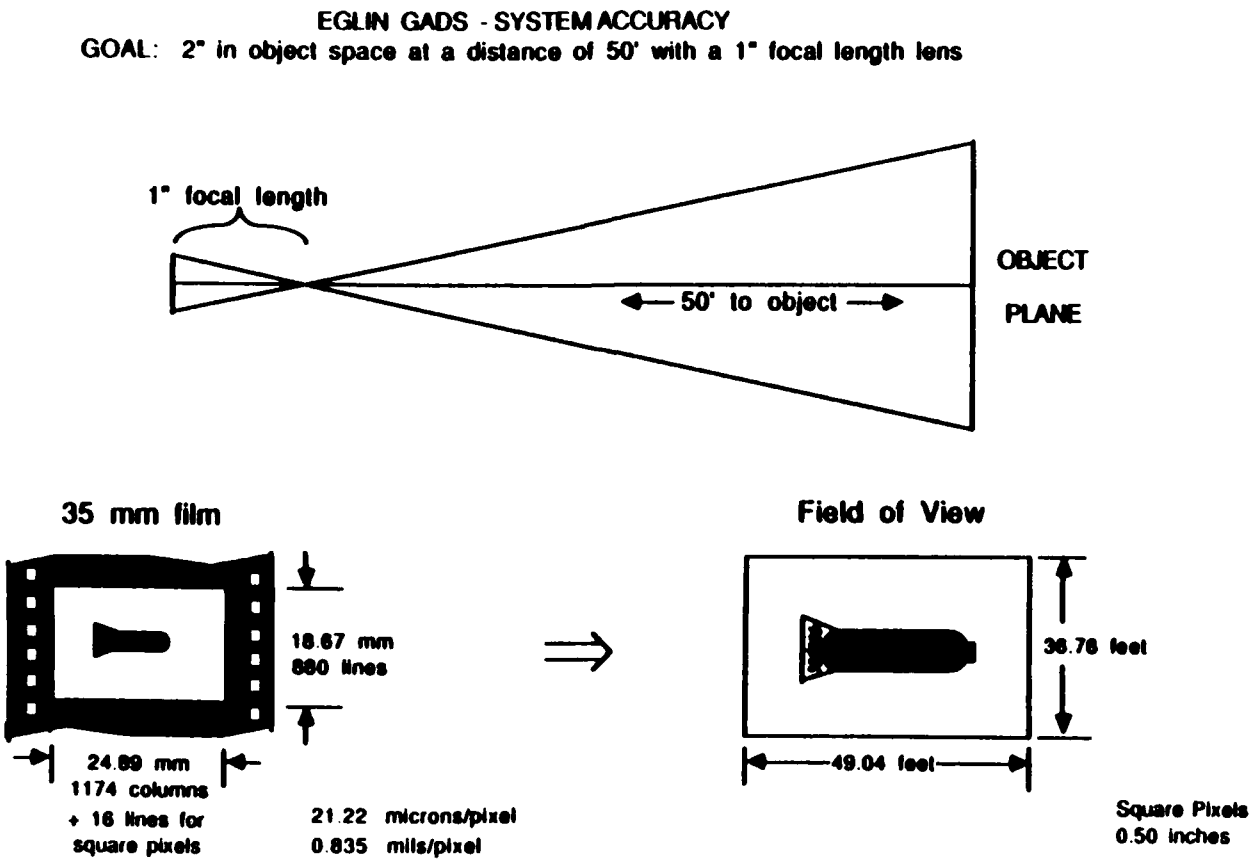

Figure 26: Geometry for 35mm Film